Matematisk-fysiske Meddelelser
udgivet af
Det Kongelige Danske Videnskabernes Selskab
Bind **34,** nr. 15

Mat. Fys. Medd. Dan. Vid. Selsk. **34,** no. 15 (1966)

A SIMPLE NONBINARY SCATTERING MODEL APPLICABLE TO ATOMIC COLLISIONS IN CRYSTALS AT LOW ENERGIES

BY

HANS HENRIK ANDERSEN

AND

PETER SIGMUND

København 1966
Kommissionær: Ejnar Munksgaard

Synopsis

This paper presents the solution of a special scattering problem which may be important in the theory of slowing-down of atomic particles in crystals. A projectile moves along the center axis of a regular ring of n equal atoms which are free and do not interact with each other. The interaction between the projectile and each ring atom is described by a Born-Mayer potential, and the scattering is assumed to be elastic and governed by the classical equations of motion. Because of symmetry, the problem can be reduced to plane motion of a particle in a potential of elliptic symmetry. The elliptic force field is approximated by a spherical one, which is dependent on the initial conditions of the individual scattering problem. For the spherical symmetrical potential, scattering angles and related quantitites have been tabulated, but simple analytical approximations can be used too. As a result, one obtains the asymptotic velocities of the ring atoms as well as the energy loss of the projectile. Furthermore, it can be decided whether the projectile is reflected by the ring. Both the feasibility of assumptions specifying the problem and the validity of different approximations made in the transformation from the elliptic to the spherical potential are investigated. Special attention is paid to proper definitions of collision time and collision length which are important in collisions in crystals. Limitations to classical scattering arising from the uncertainty principle prove to be more serious than assumed previously. Inelastic contributions to the energy loss can easily be included. The oscillator forces binding lattice atoms turn out to influence the scattering process only at very small energies. The validity of the so-called momentum approximation and a related perturbation method are also investigated.

PRINTED IN DENMARK
BIANCO LUNOS BOGTRYKKERI A-S

CONTENTS

§ 1. Introduction

The slowing-down of an atom in a crystal is a many-body problem. The concept of mean free path, governing collisions in gases, is much less significant in solids because of the high density of scattering centres. The mean free path for elastic collisions with appreciable relative energy transfer is comparable to the interatomic distance except for energies considerably up in the keV region, dependent on mass and atomic number of projectiles and substance atoms involved. At these high energies, the majority of collisions are soft ones, so that perturbation methods may be successful. At low energies all collisions are more or less hard ones, so that the perturbation approach breaks down. As a consequence of the mean free path being so small, correlations between successive collisions, due to the regular lattice structure cannot be neglected in low energy collision theory.

Two main lattice structure effects on slowing-down have been proposed. Ion bombardment of single crystals parallel to low-indexed directions might result in almost completely suppressing close collisions by keeping projectiles a certain minimum distance away from lattice rows and planes (channelling). The experiments are usually done at energies from 1 keV up to several MeV, so that a theoretical treatment can make use of perturbation methods. But, for interpretation of range distributions and especially the so-called "super tails" it is important to investigate the slowing-down mechanism at the low energy end, to know whether the projectiles come to rest at lattice sites or interstitial positions, and, finally, whether they create defects or not. From this, one might also get information on possible diffusion following the slowing-down process.

It has furthermore been proposed that lattice geometry causes a high probability of nearly head-on (replacement) collisions for knock-on atoms. It seems difficult to verify this effect experimentally, but a great variety of sputtering and radiation damage phenomena are explained in a plausible way

by assuming it to exist. According to computer simulations of slowing-down, low energy knock-on atoms act preferably by exciting collision sequences along close-packed directions without travelling far away from their starting positions.

The characteristic difficulties of a many-body problem arise as soon as a collision is neither soft nor a pure two-body event. But the many-body problem might be simplified in special cases. Both in collision sequences and channelling *almost symmetrical* orbits between and parallel to lattice rows are supposed to have an appreciable statistical weight within certain energy intervals. Therefore, calculations of *perfectly symmetric* motion might answer some of the questions raised above.

This paper presents the treatment of a simple model. A set of lattice rows is resolved into symmetric rings; the projectile moves along their common symmetry axis, and its *interaction with one ring of atoms is considered to be the basic event*. Under certain simplifying assumptions it is possible to reduce this problem to scattering of one particle in a fixed force field, which can be solved approximately.

The accuracy of approximations as well as the limitations of classical elastic scattering and the applicability to collisions in crystals are examined. The main uncertainty entering the model is the interatomic potential. The repulsive Born-Mayer potential is used throughout the paper, mainly because of simplicity and for comparison with other investigations. As far as possible, the results are discussed without specifying potential constants too strictly.

The model gives rather definite answers on the break-down of perturbation theory and the maximum elastic energy transfer. Furthermore, it is possible to define a collision length in order to estimate the overlap between successive events. Finally, some suggestions are made about the approximate treatment of non-symmetric many-body collisions.

The present paper contains the general theory. It deals with the specification of the model and some direct consequences (§ 2); several methods of reduction to spherical scattering are examined in § 3; general results such as transferred energies and scattering angles are discussed in § 4, both numerically and analytically; this chapter also deals with the concept of collision length as well as the validity of approximations made in § 3; the last chapter is dedicated to the question of applicability of the model to collisions in crystals and to a discussion of quantum corrections and inelasticity. Applications to channelling and collision sequences will be contained in a forth-coming paper.

§ 2. The Model

2.1 Basic definitions

The dynamics of the following system (ANDERSEN & SIGMUND, 1965 a) will be investigated:

1) n atoms $i = 1 \ldots n$ of mass m_1, neither bound by external forces nor interacting with each other, form initially a regular ring with radius L.
2) A projectile of mass m_0 moving on the ring axis with an initial velocity $\vec{v}_0$ (Fig. 1) interacts with the ring atoms via some repulsive potential

$$V(r_{0i}) = V(|\vec{r}_0 - \vec{r}_i|). \tag{2.1.1}$$

In applications only Born-Mayer interaction

$$V(r) = Ae^{-r/a} \tag{2.1.2}$$

will be used.
3) The collision is treated by classical mechanics.

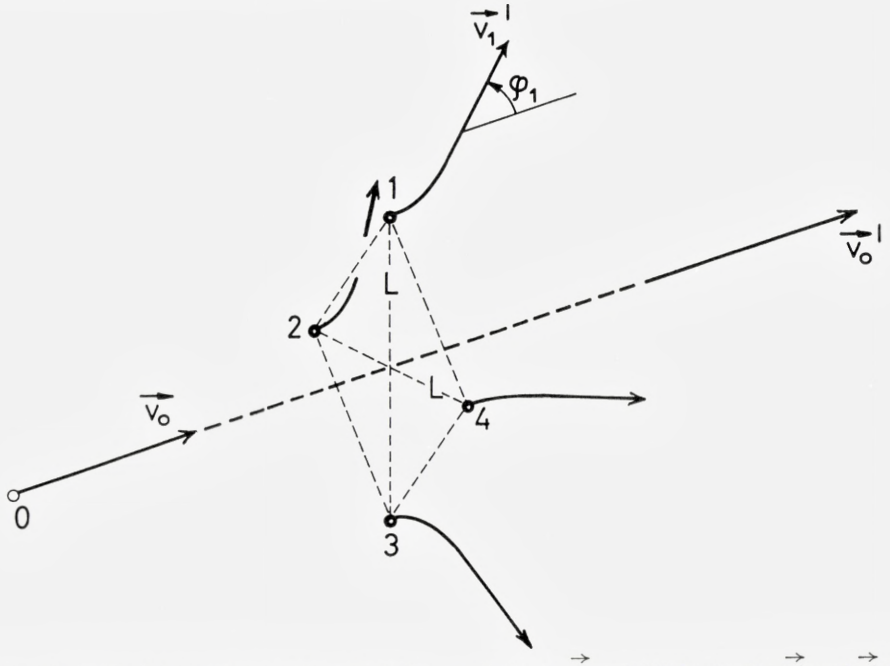

Fig. 1. Projectile 0 interacting with a ring of $n = 4$ atoms. $\vec{v}_0$ = initial velocity. $\vec{v}_0'$ and $\vec{v}_1'$ final velocities of projectile and ring particle 1.

Due to the symmetrical initial conditions the projectile will keep on moving on the ring axis, and ring atoms perform identical motions in planes made up by the axis and their initial positions (Fig. 1). Quantities of interest are:

i) the total energy loss ΔE of the projectile to the ring,
ii) the asymptotic orbits and energies of ring particles,
iii) the energy limit below which the projectile will be reflected by the ring, and
iv) the collision time and corresponding path length.

The feasibility of the assumptions involved in 1)–3) will be examined in later sections of this paper. The validity of assumption 1) depends on the role of binding forces (sect. 5.3). The significance of Born-Mayer repulsion and the choice of constants A, a is discussed in a separate paper (Andersen & Sigmund, 1965 b). Quantum mechanical limitations and inelastic effects are mentioned in sects. 5.1 and 5.2.

In applications to collisions in crystals, the ring radius L will be at least one half nearest neighbour distance ($L \gtrsim 1$Å), n may take the values 2, 3, and 4, a is supposed to be slightly smaller than one half Bohr-radius ($a \sim 0.2$Å), while A varies over a wide range of energies in the keV region, dependent on the atoms involved. Initial energies of interest range from about 10 eV up to 10 keV.

2.2 The perturbation approach

If the energy loss ΔE is very small compared to the initial energy E_0 of the projectile, ΔE can be calculated by first order perturbation theory (momentum approximation; for brevity: MA)

$$\Delta E = n \cdot \frac{1}{2m_1} \left(\int_{-\infty}^{\infty} \frac{dx_0}{v_0} \operatorname{grad}_\perp V(r_{01}) \right)^2, \tag{2.2.1}$$

where $\operatorname{grad}_\perp$ indicates the component of the force perpendicular to the orbit of the projectile. This orbit is assumed to be a straight line, while particle 1 is considered as being fixed during the collision.

For Born-Mayer interaction (2.1.2) one gets (Brinkmann, 1954)

$$\Delta E = n \cdot \frac{m_0}{m_1} \frac{A^2}{E_0} \left[\frac{L}{a} K_0 \left(\frac{L}{a} \right) \right]^2. \tag{2.2.2}$$

The function $K_0(\xi)$ is a modified Hankel function with the asymptotic expansion (JAHNKE et al., 1960)

$$K_0(\xi) \sim \sqrt{\frac{\pi}{2\xi}}\, e^{-\xi} \quad \text{for large } \xi. \tag{2.2.3}$$

According to the previous section,

$$\xi = L/a \gtrsim 5. \tag{2.2.4}$$

For these arguments the expansion (2.2.3) approximates K_0 with an accuracy better than 3 pct.

At small energies ΔE becomes large according to (2.2.2), so this approach must break down. In order to estimate the applicability of (2.2.2) we note that ΔE cannot be greater than either the initial energy E_0 or the height of the potential barrier at the ring center, so

$$\Delta E \leqq E_0 \tag{2.2.5}$$

and

$$\Delta E \leqq nAe^{-L/A}. \tag{2.2.6}$$

E_0 must be much greater than the limiting energies defined by (2.2.5) and (2.2.6). Inserting (2.2.2) and (2.2.3) we obtain

$$E_0 \gg \left(\frac{\pi}{2}\, n\, \frac{m_0}{m_1}\, \frac{L}{a}\right)^{1/2} Ae^{-L/a} \tag{2.2.5'}$$

and

$$E_0 \gg \frac{\pi}{2}\, \frac{m_0}{m_1}\, \frac{L}{a}\, Ae^{-L/a} \tag{2.2.6'}$$

as necessary conditions for the MA to be a good approximation.

For not too different masses, the two conditions are essentially equivalent. If $m_0 \gg m_1$, (2.2.6′) is the stronger one.

LEHMANN & LEIBFRIED (1963) have derived a criterion of the same type by comparing second and first order contributions in the perturbation series for the scattering angle of merely two particles:

$$E_0 \gg \frac{1}{\sqrt{2}} \left(1 + \frac{m_0}{m_1}\right) \frac{L}{a}\, Ae^{-L/a}. \tag{2.2.7}$$

(2.2.7) is equivalent to (2.2.6′) for $m_0 \gtrsim m_1$. It is easily seen that in our case (2.2.7) cannot be the appropriate criterion as soon as $m_0 \ll m_1$; the perturbation approach is reasonable if

i) the ring particles only move a small distance away during the collision, and
ii) the deflection of the projectile is small.

The latter condition is ideally fulfilled in the ring collision, while a corresponding two-particle event with $m_0 \ll m_1$ might result in a considerable deflection of the projectile. Hence, (2.2.7) will underestimate the applicability of the MA.

Numerically, the typical limits vary from some tens of eV up to several keV, because of the strong dependence on L and on the atoms involved.

Standard scattering theory is easily carried out beyond the MA, when one deals with pure two-body collisions. Also for our model some quantities of interest may be estimated using two-body scattering theory, but this must be expected to be a poor approach to the problem[1]. A comparison to the more accurate evaluation will be made in sect. 4.6.

2.3 Conservation laws

An accurate treatment is simplified by stating the conservation laws governing our system.

The asymptotic velocities $\vec{v}_i'$ of different ring atoms (Fig. 1) and their angles φ_i with the $\vec{v}_0$-axis are equal because of symmetry:

$$|\vec{v}_i'| = v_i' = v_1'; \quad \varphi_i = \varphi_1, \tag{2.3.1}$$

where

$$\cos \varphi_i = \frac{(\vec{v}_i' \cdot \vec{v}_0)}{v_i' v_0}. \tag{2.3.2}$$

Hence, momentum and energy conservation yield

$$m_0 v_0 = m_0 v_0' + n \cdot m_1 v_1' \cos \varphi_1, \tag{2.3.3}$$

$$\frac{m_0}{2} v_0^2 = \frac{m_0}{2} v_0'^2 + n \cdot \frac{m_1}{2} v_1'^2, \tag{2.3.4}$$

$\vec{v}_0'$ being the asymptotic velocity of the projectile.

Conservation of angular and transverse momentum has been fully taken into account by stating the symmetry of the orbits.

[1] Sometimes, especially in computer calculations, the interaction is cut off at a certain distance in order to ensure the two-body nature of collisions. It is obvious that this procedure might give rise to peculiar multiple scattering effects when applied to an almost symmetric ring collision (Robinson and Oen, 1963). The completely symmetric case cannot be simplified in this way.

(2.3.3) and (2.3.4) lead to the relative energy transfer to one ring atom,

$$\Delta E_1 = \frac{m_1}{2} v_1'^2 = \frac{4 \frac{m_1}{m_0} \cos^2 \varphi_1}{\left(1 + n \frac{m_1}{m_0} \cos^2 \varphi_1\right)^2} E_0 . \tag{2.3.5}$$

The total energy loss to the ring is given by

$$\Delta E = E_0 - E_0' = n \cdot \Delta E_1 , \tag{2.3.6}$$

where E_0' is the asymptotic projectile energy; the asymptotic velocity becomes

$$v_0' = \frac{1 - n \frac{m_1}{m_0} \cos^2 \varphi_1}{1 + n \frac{m_1}{m_0} \cos^2 \varphi_1} v_0 .$$

The particle is reflected by the ring if v_0'/v_0 is negative, i. e.

$$\cos \varphi_1 > \sqrt{m_0/n m_1} . \tag{2.3.7}$$

The reverse relation to (2.3.7) does not necessarily involve that the projectile really penetrates the ring, as the ring particles have a velocity component in the forward direction. However, in many applications this component is relatively small.

Most of the quantities of interest have thus been expressed by the angle φ_1. Clearly, φ_1 is governed by the interatomic potential.

2.4 Transformation to relative coordinates

Convenient coordinates describing the internal state of the system are the ring radius and the distance of the projectile from the ring center. Let us consider the motion in a plane formed by $\vec{v}_0$ and $\vec{v}_1'$ and choose $\vec{v}_0$ as the x-axis (Fig. 2). Then,

$$\vec{r}_0 = (x_0, 0); \quad \vec{r}_1 = (x_1, y_1) . \tag{2.4.1}$$

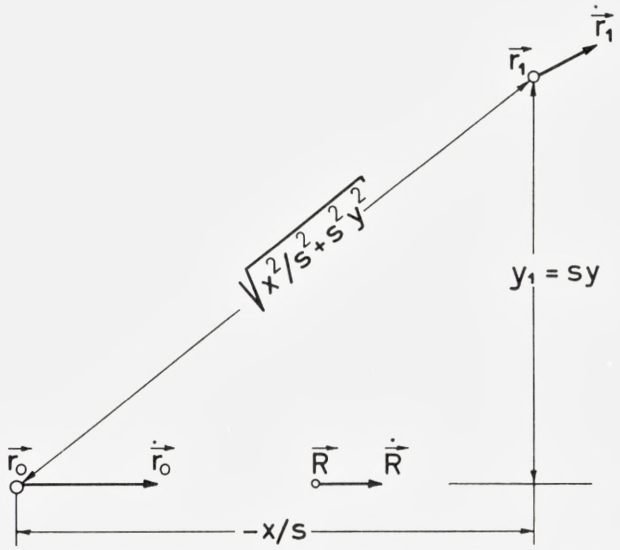

Fig. 2. Definition of relative coordinates x, y. $\vec{r}_0, \dot{\vec{r}}_0, \vec{r}_1, \dot{\vec{r}}_1$: position and velocity of projectile and *one* ring atom. $\vec{R}, \dot{\vec{R}}$: position and velocity of center-of-mass.

The center-of-mass moves along the x-axis, so

$$\vec{R} = (X, O); \quad X = \frac{m_0}{M} x_0 + n \cdot \frac{m_1}{M} x_1, \tag{2.4.2}$$

where M is the total mass:

$$M = m_0 + n m_1. \tag{2.4.3}$$

Furthermore, we define relative coordinates

$$x = s \cdot (x_0 - x_1); \quad y = y_1/s, \tag{2.4.4}$$

so that

$$x_0 = X + n \frac{m_1}{M} \cdot \frac{x}{s}; \quad x_1 = X - \frac{m_0}{M} \frac{x}{s}; \quad y_1 = sy. \tag{2.4.5}$$

In (2.4.4) we have introduced a scaling factor s. This is necessary in order to make the reduced mass isotropic. The kinetic energy

$$E_{\text{kin}} = \frac{m_0}{2}\dot{x}_0^2 + n \cdot \frac{m_1}{2}(\dot{x}_1^2 + \dot{y}_1^2)$$

becomes in the new coordinates (2.4.5)

$$E_{\text{kin}} = \frac{M}{2}\dot{X}^2 + n \cdot \frac{m_1}{2}\left(\frac{m_0}{M}\frac{\dot{x}^2}{s^2} + s^2\dot{y}^2\right).$$

This simplifies to

$$E_{\text{kin}} = \frac{M}{2}\dot{X}^2 + n\frac{m_1}{2}s^2(\dot{x}^2 + \dot{y}^2), \tag{2.4.6}$$

if we choose

$$s^4 = m_0/M = \frac{m_0}{m_0 + nm_1} < 1. \tag{2.4.7}$$

The total potential energy becomes, according to (2.1.1) and Fig. 2,

$$\Phi(x, y) = \sum_i V(r_{0i}) = nV(r_{01}) = nV\left(\sqrt{x^2/s^2 + s^2y^2}\right). \tag{2.4.8}$$

So, in the reduced scattering problem the force field has elliptical symmetry. If the projectile comes in from infinity we get the initial conditions

$$x(t = -\infty) = -\infty;$$

$$p = y(-\infty) = \frac{1}{s}y_1(-\infty) = L/s, \tag{2.4.9}$$

$$v_r = \dot{x}(-\infty) = sv_0, \tag{2.4.10}$$

$$E_r = n\frac{m_1}{2}s^2(\dot{x}^2 + \dot{y}^2)\Big|_{t=-\infty} = \frac{nm_1}{M}E_0, \tag{2.4.11}$$

where we have made use of (2.4.4), (2.4.6) and (2.4.7). The quantities p, v_r and E_r are the impact parameter, relative velocity and relative energy defining the reduced scattering problem (Fig. 3).

The relation between scattering angle ϑ in the reduced system (Fig. 3) and φ_1 is found in the following way:

$$\operatorname{tg}\varphi_1 = \frac{\dot{y}_1}{\dot{x}_1}\Big|_{t=\infty} = \frac{s^2v_0\sin\vartheta}{s^4v_0 - s^4v_0\cos\vartheta} = \frac{1}{s^2}\operatorname{ctg}\vartheta/2. \tag{2.4.12}$$

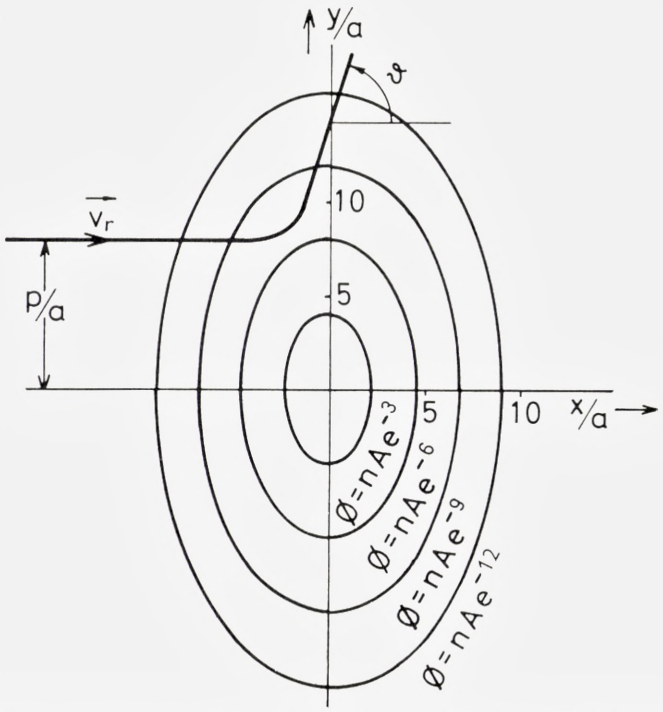

Fig. 3. The reduced scattering problem for Born-Mayer interaction. Successive equipotential lines differ by a factor of $e^{\pm 3}$. Quantitative details correspond to an example discussed in sect. 4.3 (Fig. 7).

Here we have used (2.4.5), (2.4.2) and (2.4.10). Inserting (2.4.12) into (2.3.5) we obtain the energy loss (2.3.6):

$$\Delta E = 4\frac{nm_1}{M} E_0 \cdot \sin^2\frac{\vartheta}{2}\left(1 - \frac{nm_1}{M}\sin^2\vartheta/2\right). \tag{2.4.13}$$

The condition (2.3.7) for reflection reads

$$\sin^2\vartheta/2 > \frac{M}{2nm_1}. \tag{2.4.14}$$

The projectile penetrates the ring if $\vartheta < \pi/2$, i. e.

$$\sin^2\vartheta/2 < 1/2. \tag{2.4.15}$$

In the intermediate interval,

$$\frac{1}{2} < \sin^2 \vartheta/2 < \frac{1}{2} \cdot \frac{M}{nm_1}, \tag{2.4.16}$$

the projectile moves asymptotically in the forward direction, but behind the centre of the ring.

§ 3. Reduction to Spherical Symmetry

3.1 General remarks

The reduced scattering problem is simple, but nontrivial because of the elliptical symmetry of the potential $\Phi(x,y)$. As angular momentum is not conserved, the scattering angle ϑ and related quantities cannot be expressed by integrals as in standard scattering theory. In order to calculate only the orbit of the scattered particle, it would be most convenient to start at Jacobi's principle, which states that

$$\delta \int_1^2 \sqrt{E_r - \Phi(x,y)}\, ds = 0; \tag{3.1.1}$$

where $y = y(x)$ has to be varied between two fixed points 1 and 2 in the x,y-plane, and ds is the line element

$$ds = \sqrt{1 + (dy/dx)^2}\, dx.$$

(3.1.1) is equivalent to a differential equation for $y = y(x)$:

$$\frac{1}{2} \cdot \frac{1}{E_r - \Phi} \left(\frac{\partial \Phi}{\partial y} - y' \frac{\partial \Phi}{\partial x} \right) + \frac{y''}{1 + y'^2} = 0. \tag{3.1.2}$$

Several standard procedures have been examined in order to solve (3.1.1) or (3.1.2). Most of them are rather specific for the spherical case. The only systematic approach, which was found to have some success, is the perturbation series expansion of (3.1.2). The first two terms are evaluated in Appendix A. But, as was stated by Lehmann and Leibfried (1963) for spherically symmetric interaction, the perturbation series has in general a finite radius of convergence, and higher than first order perturbations do hardly improve the scattering formula.

Instead of calculating approximate orbits in the exact field, one can also calculate exact orbits for an approximate field. The method is widely used in scattering theory and has the advantage that the limit of applicability may easily be found by comparing "true" and approximate forces.

As long as $m_0 \gtrsim m_1$, the excentricity of the potential lines is moderate. The proportion between major and minor axis: $\frac{1}{s^2} = \sqrt{1 + nm_1/m_0}$ becomes $\lesssim 2.5$. We shall mainly concentrate our attention on the case $m_0 \gtrsim m_1$, as in the opposite case, $m_0 \ll m_1$, the MA remains valid down to sufficiently low energies, given by (2.2.5′). Furthermore, deflections in strongly varying Born-Mayer fields will take place in a rather small region in space. Hence, in the case $m_0 \gtrsim m_1$ it is expected to be an excellent approximation to replace $\Phi(x,y)$ by a potential of *spherical symmetry* which is similar to Φ in a certain critical region. This critical region should be centered around that point where the scattered particle achieves its highest potential energy. Unfortunately, it is not possible to find this point in a straightforward manner when p and E_r are given.

Therefore, two complementary matching methods are discussed, which we call close collision approximation (CCA) and distant collision approximation (DCA). In both cases the center of a spherical potential is found from the radius of curvature of a certain equipotential line. CCA and DCA will be seen to cover the whole curve $\vartheta(p)$ for $o \leq p \leq \infty$ for given E_r with a good accuracy. As small impact parameters p do not occur in applications, the DCA will be the more important approach.

3.2 Close collision approximation

Figure 4 shows the orbit of a particle in an almost central collision. The closest distance of approach $R(p)$ will be approximately equal to $R(p = 0) = R_0$, which is given by

$$\Phi(-R_0, 0) = E_r. \tag{3.2.1}$$

The radius of curvature of the equipotential line in $(-R_0, 0)$ is, according to (2.4.8), given by

$$\varrho = \frac{(R_0/s^2)^2}{R_0} = \frac{R_0}{s^4}. \tag{3.2.2}$$

Hence, the centre of the CCA potential will be at

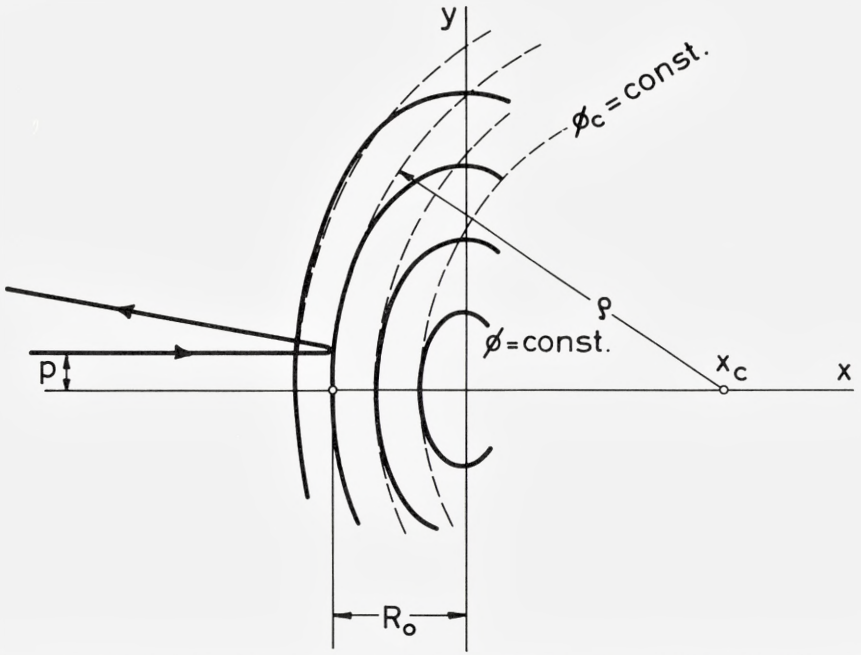

Fig. 4. Construction of the CCA potential Φ_C (schematically). For small p only the potential near $(-R_0, 0)$ causes deflection. x_C is the center of curvature to the potential line through this point.

$$x_C = -R_0 + \varrho = R_0\left(\frac{1}{s^4} - 1\right). \tag{3.2.3}$$

The CCA potential Φ_C is then constructed in such a way that

$$\Phi_C(x,y) = \Phi(x,y) \quad \text{for} \quad y = 0, \quad x \leq 0. \tag{3.2.4}$$

For the BM potential (2.1.2), $\Phi(x,y)$ is given by

$$\Phi(x,y) = nA \exp\left(-\frac{1}{a}\sqrt{x^2/s^2 + y^2 \cdot s^2}\right), \tag{3.2.5}$$

so that

$$\Phi_C(x,y) = nAe^{x_C/sa} \cdot e^{-r'/sa}, \tag{3.2.6}$$

where r' is the distance between (x,y) and $(x_C, 0)$. Hence, the scattering angle in the CCA may be expressed by that for a spherically symmetric potential

$$\Phi_C(r') = A_C e^{-r'/a_C}, \tag{3.2.7}$$

with

$$a_C = sa; \quad A_C = nAe^{x_C/sa} = E_r\left(\frac{nA}{E_r}\right)^{1/s^4}, \tag{3.2.8}$$

where we have made use of (3.2.1) and (3.2.3). Obviously, Φ_C yields the exact solution for the central collision. The validity of this approach at finite impact parameters will be investigated in sects. 4.3 and 4.5.

3.3 Distant collision approximation

In distant collisions, where ϑ is small, the scattering will essentially take place near the point $(0,p)$. We can therefore choose the center of curvature of the potential line through this point as symmetry center of another matching potential Φ_D, as indicated in Fig. 5. The radius of curvature ϱ is given by

$$\varrho = \frac{(ps^2)^2}{p} = ps^4, \tag{3.3.1}$$

and the symmetry center has the ordinate

$$y_D = p - \varrho = p(1 - s^4). \tag{3.3.2}$$

Φ_D is chosen so that

$$\Phi_D(x,y) = \Phi(x,y) \quad \text{for} \quad x = 0, \quad y \geq y_D. \tag{3.3.3}$$

Using (3.2.5), we get

$$\Phi_D = n \cdot A \cdot e^{-\frac{sy_D}{a}} \cdot e^{-\frac{sr'}{a}},$$

where r' is now the distance between (x,y) and $(0,y_D)$. Hence, the DCA potential is given by

$$\Phi_D(r') = A_D e^{-r'/a_D}, \tag{3.3.4}$$

where

$$a_D = \frac{a}{s} \tag{3.3.5}$$

and

$$A_D = n \cdot A \cdot e^{-\frac{sy_D}{a}} = nAe^{-\frac{sp}{a}(1-s^4)}. \tag{3.3.6}$$

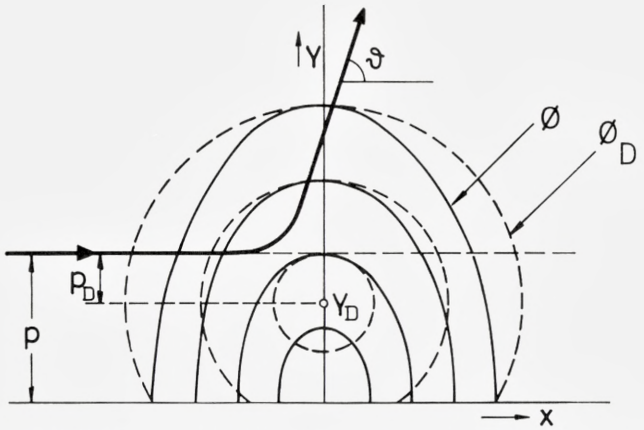

Fig. 5. Construction of the DCA potential Φ_D. For small scattering angle ϑ mainly the potential near $(0, p)$ causes deflection. y_D is the center of curvature of the potential line through this point. Quantitative details correspond to the example discussed in sect. 4.3 (Fig. 7).

Contrary to the CCA we also get a new impact parameter in the DCA. Instead of p we have (Fig. 5)

$$p_D = \varrho = ps^4. \tag{3.3.7}$$

The scattering angle is determined by the two proportions

$$\frac{p_D}{a_D} = s^4 \cdot \frac{L}{a}; \quad \frac{E_r}{A_D} = \frac{m_1}{M} \frac{E_0}{A} e^{\frac{L}{a} \cdot \frac{nm_1}{M}}. \tag{3.3.8}$$

Deriving (3.3.8) we have used (2.4.9), (2.4.11) and (2.4.7).

Also the applicability of this approach will be examined in sections 4.3 and 4.5.

3.4 Constant velocity approximation

A much simpler reduction to spherical scattering is found in the case $m_0 \gg nm_1$, where the projectile moves nearly uniformly independent of the interaction potential. In this case it seems reasonable to go over to a system moving with velocity v_0 and to consider the projectile as a fixed scattering center in this system. As the ring particles are independent of each other, they are scattered individually by an angle α (Fig. 6), which can be cal-

culated from the *true* Born-Mayer potential as interaction, impact parameter L and energy

$$E' = \frac{m_1}{m_0} E_0 . \tag{3.4.1}$$

In the laboratory system, particle 1 has, after the collision, velocity components

$$\left.\begin{aligned} v'_{1x} &= v_0(1 - \cos\alpha) \\ v'_{1y} &= v_0 \sin\alpha , \end{aligned}\right\} \tag{3.4.2}$$

corresponding to a scattering angle φ_1 given by

$$\operatorname{tg}\varphi_1 = \frac{\sin\alpha}{1-\cos\alpha} = \operatorname{ctg}\alpha/2 , \tag{3.4.3}$$

and an energy

$$\Delta E_1 = 4\frac{m_1}{m_0} E_0 \cdot \sin^2\alpha/2 . \tag{3.4.4}$$

An approach of this kind has been used by WEIJSENFELD (1964) in the theory of assisted focusing collision sequences. The essential difference to the MA is that the ring particles are not considered to be fixed during the collision. They are free to move away, while the projectile is restricted in its transversal motion. This approach, which we call constant velocity approximation (CVA), is a perturbation approach in the sense that the deflection of the ring particles is determined by the zero order motion of the projectile. The approximation does, however, not involve an expansion in powers of the interaction potential. It will turn out in sect. 4.3 that the quality of the CVA is surprisingly good, even for lighter projectiles.

When m_0 is of the order of nm_1, the CVA violates the conservation laws. Weijsenfeld avoided this by assuming only the y-component v'_{1y} to be determined by (3.4.2), while the x-component is found from energy and momentum conservation. However, for not too large energy transfers the two formulations are essentially equivalent, as the ring particles move almost perpendicularly to $\vec{v}_0$. The straightforward formulation of the Weijsenfeld approach gives an energy transfer

$$\Delta E_1 = 4\frac{m_1}{m_0} E_0 \sin^2\alpha/2\left(1 + 2n\frac{m_1}{m_0}\sin^4\frac{\alpha}{2} + \ldots\right) \tag{3.4.5}$$

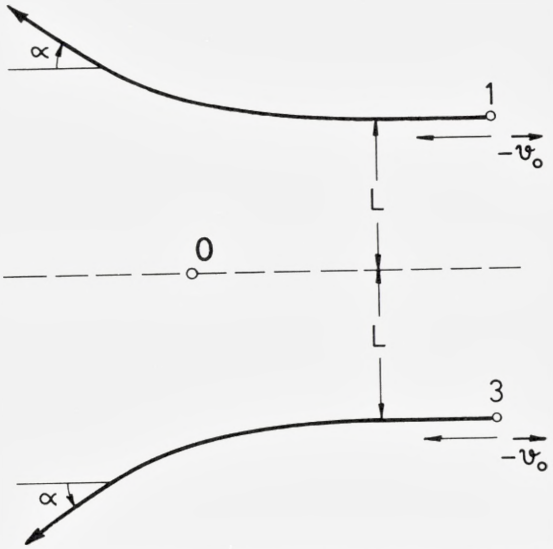

Fig. 6. Constant velocity approximation. The situation in Fig. 1 is considered from a system moving with $\vec{v}_0$. The projectile 0 is assumed to be at rest in this system throughout the collision.

which differs from (3.4.4) only by a correction term of fourth order in $\sin \alpha/2$, which is negligible. We prefer to use the CVA, as it is much simpler than Weijsenfeld's original approach. As it will turn out in sect. 4.3, the CVA may even be valid if ΔE_1 is not negligible compared to E_0.

§ 4. Application to Born-Mayer Interaction

4.1 Accurate scattering angles

We have now found three possibilities of reducing the original problem of finding φ_1 to that of calculating the scattering angle

$$\vartheta(E',p') = \pi - \int_{r'_m}^{\infty} \frac{2p'dr'/r'^2}{\sqrt{1 - \Phi'(r')/E' - (p'/r')^2}}, \tag{4.1.1}$$

for some spherical Born-Mayer potential

$$\Phi'(r') = A'e^{-r'/a'}. \tag{4.1.2}$$

E' and p' indicate relative energy and impact parameter in any of the three spherical scattering problems. r'_m is the distance of closest approach defined by the zero of the square root in (4.1.1).

The integral (4.1.1) has been tabulated by Robinson (1963) for $0.005 \leq E'/A' \leq 1$ and p'/a' ranging from zero up to such values where the accuracy of the MA is sufficiently good. The tables provide enough points to cover all cases of interest in applications as far as concerns the DCA, which is the approximation mostly used later on. Therefore, in plotting ΔE vs. E_0, uncertainties from the evaluation of (4.1.1) can be assumed to be negligible within the range of validity of the DCA.

For those cases where the tables do not provide data one has to use analytical approximations. A list of references has been given in an earlier paper (Sigmund & Vajda, 1964). We only mention two formulae, the most accurate one given by Heinrich (1964):

$$\sin \vartheta/2 = \frac{1}{1 + 2/\vartheta_1}, \tag{4.1.3}$$

where

$$\vartheta_1 = \frac{A'}{E'} \cdot \frac{r_m'^3}{a' p'^2} K_0(r'_m/a'). \tag{4.1.4}$$

It is seen by expansion that (4.1.3) gives the correct result at small angles. Furthermore, $\vartheta(p' = 0) = \pi$, as it must be. Within the whole range of the numerical tables the accuracy of (4.1.3) is better than 4 pct. The disadvantage of this formula is that r'_m is defined by a transcendental equation, so one has to use p' and r'_m as independent variables and calculate E'.

At large angles the following formula has proved to be a good approximation (Sigmund & Vajda, 1964):

$$\sin^2 \vartheta/2 = \frac{1 - \left(\frac{p'}{R'_0}\right)^2 \left(1 - \frac{a'}{R'_0}\right)^2}{1 + 4 \frac{a'}{R'_0} \cdot \left(\frac{p'}{R'_0}\right)^2}, \tag{4.1.5}$$

where R'_0 is the head-on radius defined by

$$\frac{R'_0}{a'} = \ln \frac{A'}{E'}. \tag{4.1.6}$$

(4.1.5) is based on the matching method of Leibfried & Oen (1962).

4.2 A simple analytical approximation

For qualitative considerations the above mentioned scattering formulae are too complex. If one is not interested in a high accuracy, an extremely simple approximation may be found as follows. The potential (4.1.2) is matched by a cut-off Coulomb potential:

$$\Phi_M(r') = \begin{cases} C\left(\frac{c}{r'} - 1\right) \ldots\ldots\ldots & r' < c \\ 0 \qquad\qquad \ldots\ldots\ldots & r' \geq c. \end{cases} \tag{4.2.1}$$

The constants C and c are chosen so that the potentials agree in value and slope at $r' = p'$:

$$\Phi_M(p') = \Phi'(p') \quad \text{and} \quad \frac{d}{dp'}\Phi_M(p') = \frac{d}{dp'}\Phi'(p'). \tag{4.2.2}$$

This matching method is similar to those by Leibfried & Oen (1962) and Lehmann & Robinson (1964); Leibfried and Oen fulfilled the conditions (4.2.2) in $r' = R_0'$ instead of $r' = p'$, and Lehmann and Robinson matched in $r' = r_m'$. For the very central collision ($p' \ll R_0'$) our matching procedure is expected to break down.

Potential (4.2.1) yields, according to Leibfried and Oen,

$$\sin^2\frac{\vartheta}{2} = \frac{1 - (p'/c)^2}{1 + \left(\frac{p'}{c}\right)^2 \cdot \frac{4E'}{C}\left(\frac{E'}{C} + 1\right)} \quad \text{for} \quad p' < c.$$

From (4.2.2),

$$c = \frac{p'^2}{p' - a'}; \quad C = A' e^{-p'/a'}\left(\frac{p'}{a'} - 1\right),$$

so

$$\sin^2\frac{\vartheta}{2} = \frac{2\frac{p'}{a'} - 1}{\left(\frac{p'}{a'} + 2\frac{E'}{A'}e^{p'/a'}\right)^2 - 4\frac{E'}{A'}e^{p'/a'}}, \tag{4.2.3}$$

We shall mainly apply (4.2.3) in connection with the DCA. According to (3.3.8), we have

$$\frac{p_D}{a_D} = s^4 \cdot \frac{L}{a} \gtrsim \frac{1}{5} \cdot 5 = 1 \quad \text{for} \quad m_0 \gtrsim m_1,$$

when we use the numerical estimates of sects. 2.1 and 3.1. Comparison with the numerical tables shows that the accuracy of (4.2.3) is better than 10 pct. for $p'/a' \gtrsim 1.5$. For the very lowest values of p_D/a_D one has to use more careful estimates. Clearly, (4.2.3) becomes wrong for $p' < a'$. Inserting (3.3.8) in (4.2.3) we obtain

DCA:
$$\sin^2 \frac{\vartheta}{2} = \frac{2 \frac{m_0}{M} \frac{L}{a} - 1}{\left(\frac{m_0}{M} \frac{L}{a} + 2 \frac{m_1}{M} \frac{E_0}{A} e^{L/a} \right)^2 - 4 \frac{m_1}{M} \frac{E_0}{A} e_{L/a}}. \tag{4.2.4}$$

4.3 General results

In order to give an impression of the applicability of the different approximation methods we discuss an example. Fig. 7 shows $\sin \vartheta/2$ as a function of L/a for $n = 2$; $m_0 = m_1$; $E_0/A = 4.45_{10}-3$. For the copper potential of Gibson et al. (1960),

$$A = 22.5 \text{ keV}; \quad a = .196 \text{ Å} \quad \text{for} \quad \text{Cu}, \tag{4.3.1}$$

this corresponds to $E_0 = 100$ eV. The calculations were done in the following way:

CCA: Parameters from (3.2.8), $\sin \vartheta/2$ a) from (4.1.3), b) from (4.1.5) (4.3.2)

DCA: Parameters from (3.3.8), $\sin \vartheta/2$ from numerical tables (Robinson, 1963) (4.3.3)

MA: $\vartheta = (\text{tg}\vartheta)^{(1)}$ from (A. 8) (4.3.4)

CVA: ϑ from (2.4.12), where φ_1 is given by (3.4.3) and α is taken from the numerical tables. (4.3.5)

As the CVA has no connection to the elliptical scattering problem, the reduced scattering angle ϑ introduced by (4.3.5) has only formal significance. It is plotted in Fig. 7 in order to show the direction of discrepancies.

We know that the CCA and MA are correct at, respectively, small and large impact parameters. Fig. 7 indicates that the DCA not only yields the

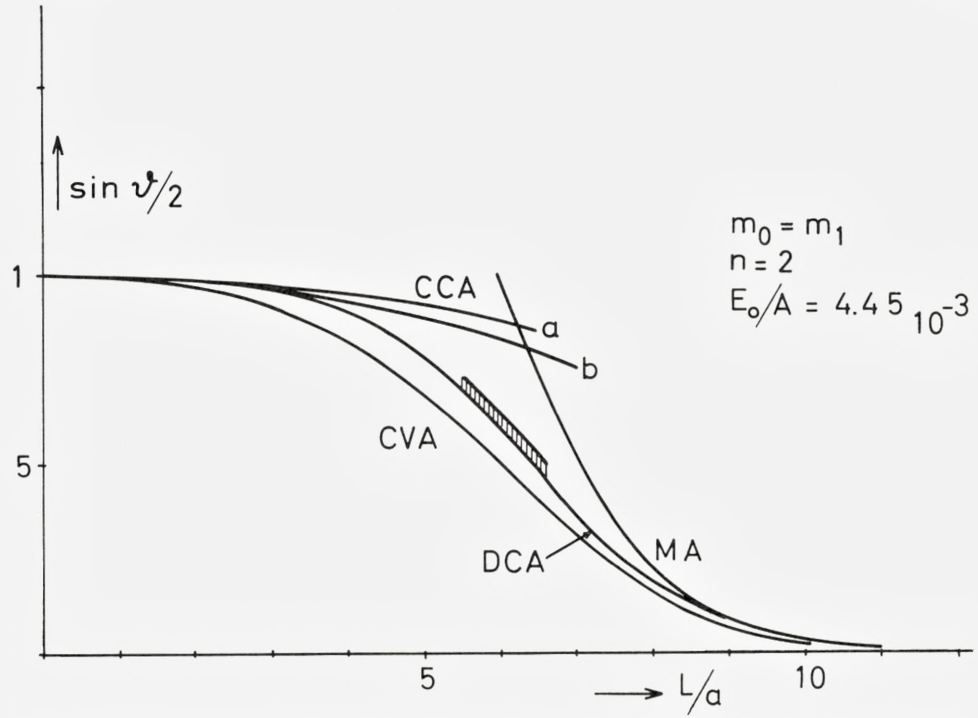

Fig. 7. Comparison of scattering angles in the reduced system, obtained by different approximations discussed in § 3. $\vartheta(p)$ passes probably through the shaded area in the region where the approximations differ most drastically (sect. 4.5).

asymptotic behaviour in these extremal cases (in Fig. 7: $L/a \lesssim 3$ and $L/a \gtrsim 8$), but also represents a plausible interpolation in the region where the discrepancy between the four curves is greatest (in Fig. 7: $5 \lesssim L/a \lesssim 7$). We note that it is just this interval of L/a which is extremely important in applications.

It will be shown in sect. 4.5 that the DCA slightly underestimates ϑ and that the correct ϑ-curve most probably lies in the shaded region.

We note that $s^4 = 1/3$ in this example. For s^4 closer to 1, the quality of the DCA is expected to be better, as this approach yields the exact solution for $s^4 = 1$. Let us, therefore, look at another example, where s^4 is much smaller.

In applications we are mainly interested in the dependence of ΔE on E_0 at a fixed ring radius L. ΔE is found from (2.4.13). We consider the case (Fig. 8)

$$n = 2; \quad \frac{m_0}{m_1} = \frac{20}{64}; \quad \frac{L}{a} = 6.5; \quad A = 10.1 \text{ keV}, \tag{4.3.6}$$

where $s^4 = 0.135$. (4.3.6) might represent a neon ion interacting with two nearest neighbour atoms in a copper crystal under the assumption that (4.3.1) properly describes the interaction between copper atoms (ANDERSEN & SIGMUND, 1965 b).

It appears that ΔE is reasonably approximated by the DCA over the whole range of energies E_0. This curve agrees with the MA at high energies ($E_0 \gtrsim 100$ eV), it goes through a maximum somewhat smaller than the potential barrier (30 eV) so that condition (2.2.6) is fulfilled. Below the maximum ΔE approaches the straight line $\Delta E = E_0$ corresponding to total stopping, and at still smaller energies the curve bends away from $\Delta E = E_0$, corresponding to reflection (2.3.7). Only at very low energies ($E_0 \ll 10$ eV) does DCA agree with CCA.

The CVA appears to be a poor approach in this case, which is due to the small mass ratio $m_0/nm_1 = 0.156$. On the other hand, the MA appears to be valid almost down to $E_0 = 50$ eV. Because of their big masses, the ring atoms can be considered as remaining at their lattice sites during the collision, so that condition i) in sect. 2.2 is fulfilled.

An analytical evaluation is possible for not too small projectile masses ($m_0 \gtrsim nm_1/2$). We insert the simple formula (4.2.4) into (2.4.13). Exact determination of the maximum of ΔE would be rather complicated because of the last factor in (2.4.13). Fortunately, this is slowly varying and close to 1 near the maximum as will be seen. If we neglect it for the determination of the maximum we obtain by differentiation

$$E_0(\max) = \frac{m_0}{2m_1} \cdot \frac{L}{a} A e^{-L/a}. \tag{4.3.7}$$

The energy transfer at $E_0(\max)$ becomes then

$$\Delta E(\max) \approx \Delta E\big(E_0(\max)\big) = nAe^{-L/a}\left(1 - \frac{nm_1}{2m_0}\frac{a}{L}\right). \tag{4.3.8}$$

(4.3.8) states that a heavy projectile ($m_0 \gg m_1$) is able to dissolve the ring almost completely during the collision, i. e. to transform the potential barrier $nAe^{-L/a}$ into kinetic energy of ring atoms.

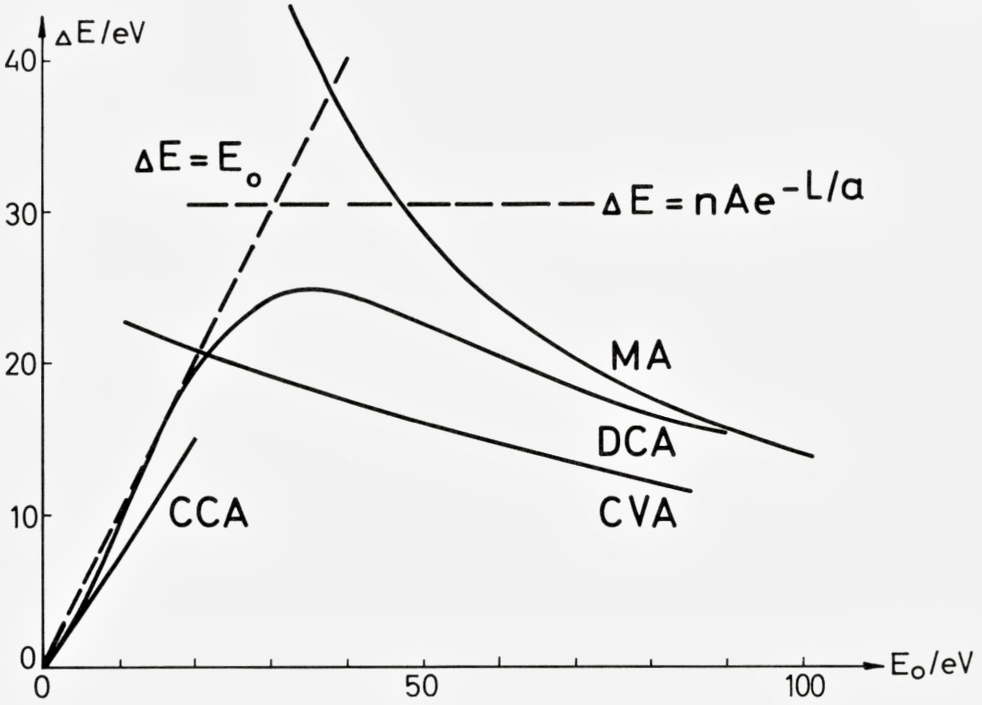

Fig. 8. ΔE vs. E_0 for $n = 2$; $\frac{m_0}{m_1} = \frac{20}{64}$; $s^4 = 0.135$, $L/a = 6.5$; $A = 10.1$ keV (Ne in Cu).

As soon as the term $\frac{nm_1}{2m_0}\frac{a}{L}$ becomes comparable to 1 (if $m_1 \gg m_0$), $\Delta E(\max)$ will be greater than (4.3.8) but, of course, smaller than the potential barrier. A more accurate analytical determination is, however, doubtful in view of the approximate character of the scattering formula (4.2.3). The error in (4.3.8) is by comparison to correct evaluation of the DCA found to be smaller than 25 pct. for $s^4 > .25$.

The complete function $\Delta E(E_0)$ becomes

$$\Delta E = nAe^{-L/a}\frac{4\xi(1-\beta/2)}{(1+\xi)^2 - 2\beta\xi}\left(1 - \frac{nm_1}{M}\frac{\beta(1-\beta)}{(1+\xi)^2 - 2\beta\xi}\right), \qquad (4.3.9.)$$

where

$$\xi = E_0/E_0(\max); \quad \beta = \frac{M}{m_0}\frac{a}{L}. \qquad (4.3.10)$$

Especially for $m_0 \gg m_1$, $\beta \ll 1$ so

$$\Delta E \approx nAe^{-L/a} \frac{4\xi}{(1+\xi)^2} \quad \text{for} \quad \xi \gtrsim 1. \tag{4.3.11}$$

This is a very important formula as it covers a region where the MA overestimates ΔE strongly. Inserting (4.3.7) into (2.2.2) and using (2.2.3) one would obtain

$$\text{MA:} \qquad \Delta E\big(E_0(\max)\big) = \pi nAe^{-L/a}, \tag{4.3.12}$$

which differs from (4.3.8) by a factor of π. It is characteristic for the case $m_0 \gg m_1$ that the maximum of ΔE is extremely broad. According to (4.3.11), ΔE drops to $\Delta E(\max)/2$ at $\xi = 5.8$. It should be mentioned that (4.3.11), within the mentioned accuracy of about 25 pct., also describes ΔE for $E_0 < E_0(\max)$.

While the MA fails completely for heavy projectile masses, $m_0 \gg m_1$, the CVA is supposed to be a good approximation. Evaluating (3.4.4) by use of (4.2.3) we obtain

$$\text{CVA:} \quad \Delta E = n\Delta E_1 = nAe^{-L/a} \frac{4\left(1 - \dfrac{a}{2L}\right)\xi}{(1+\xi)^2 - 2\xi\dfrac{a}{L}} \quad \text{for} \quad m_0 \gg m_1. \tag{4.3.13}$$

For $m_0 \gg m_1$, one gets $\beta \approx a/L$, so (4.3.13) agrees with (4.3.9), apart from the last factor in (4.3.9), which is small for $\xi > 1$.

The discussion of laboratory scattering angles is postponed to sect. 4.6. Here we examine the question whether the projectile will be reflected. At first we note that the condition (2.4.14) cannot be fulfilled as soon as

$$M \geq 2nm_1 \quad \text{or} \quad m_0 \geq nm_1. \tag{4.3.14}$$

This means that a heavy projectile penetrating a series of concentric rings of free, light atoms along their common axis will never be stopped completely. In a crystal, of course, the binding of ring atoms and thermal scattering will prevent this kind of "hyperchannelling". For $m_0 \leq nm_1$, the projectile will be reflected if its energy is smaller than a certain limiting energy E_{refl} corresponding to a critical scattering angle (2.4.14)

$$\sin^2 \vartheta_{\text{refl}}/2 = \frac{1}{2}\left(1 + \frac{m_0}{nm_1}\right), \tag{4.3.15}$$

$\vartheta_{\mathrm{refl}}$ is always greater than $\pi/2$. For these angles the Born-Mayer scattering law is well approximated by (4.1.5). Inserting (3.2.8) and (3.3.8) into (4.1.5) and neglecting $a'/R_0' \ll 1$ we obtain

$$\text{CCA:}\quad E_{\mathrm{refl}} \approx nA\left(1+\frac{m_0}{nm_1}\right)\exp\left(-\frac{L}{a}\sqrt{\frac{2nm_1m_0}{n^2m_1^2-m_0^2}}\right). \tag{4.3.16}$$

$$\text{DCA:}\quad E_{\mathrm{refl}} \approx nA\left(1+\frac{m_0}{nm_1}\right)\exp\left(-\frac{L}{a}\left(\frac{nm_1}{M}+\frac{m_0}{M}\sqrt{\frac{2nm_1}{nm_1-m_0}}\right)\right). \tag{4.3.17}$$

For $m_0 \ll nm_1$, (4.3.17) gives the expected result

$$E_{\mathrm{refl}} \approx nAe^{-L/a}, \tag{4.3.18}$$

namely, the potential barrier. $\vartheta_{\mathrm{refl}}$ is about $\pi/2$ in this case, so the CCA is not expected to give reliable ϑ-values.

For $m_0 \approx nm_1$, where $\vartheta_{\mathrm{refl}} \approx \pi$, the CCA yields

$$E_{\mathrm{refl}} \approx 2nA\exp\left(-\frac{L}{a}\sqrt{\frac{m_0}{nm_1-m_0}}\right). \tag{4.3.19}$$

This energy might become very small, hence the validity of (4.3.19) is limited again because of the role of binding forces (sect. 5.3).

The condition (2.4.15) for penetration is only evaluated in the DCA. Analogous to (4.3.17) one obtains

$$\text{DCA:}\quad E_{\mathrm{pen}} = nA\left(1+\frac{m_0}{nm_1}\right)\exp\left(-\frac{L}{a}\left(\frac{nm_1}{M}+\sqrt{2}\,\frac{m_0}{M}\right)\right). \tag{4.3.20}$$

Obviously, for $m_0 \ll m_1$,

$$E_{\mathrm{pen}} = nAe^{-L/a}, \tag{4.3.21}$$

as it must be.

4.4 Collision Length and Time Integral

The concept of collision length, which is a path length travelled during the collision, is needed both for the problem of overlap between successive impacts, the role of binding forces (sect. 5.3) and the validity of matching potentials (next section). The fundamental formulae will be derived in this section.

Let us start by considering a reduced system with fixed, spherical Born-Mayer potential and use the notations from sect. 4.1.

Within the limits of the MA, the flying particle (m' = mass, v' = velocity) transfers the total momentum

$$\Delta p = \frac{2A'}{v'} \cdot \sqrt{\frac{\pi p'}{2 a'}}\, e^{-p'/a'}, \quad \text{for} \quad \frac{p'}{a'} \gg 1, \tag{4.4.1}$$

to the scattering center. We define a collision time $\Delta\tau'$ by the relation

$$\Delta p = F_{\max} \cdot \Delta\tau', \tag{4.4.2}$$

where $F_{\max}$ represents the force acting at the closest approach, i. e.

$$F_{\max} = \frac{A'}{a'} e^{-p'/a'} \tag{4.4.3}$$

for a particle moving on a straight line. Comparing (4.4.1), (4.4.2) and (4.4.3) we have to choose

$$\Delta\tau' = \frac{1}{v'} \sqrt{2\pi a' p'}. \tag{4.4.3}$$

This corresponds to a collision length

$$\Lambda' = \sqrt{2\pi a' p'}. \tag{4.4.4}$$

It is characteristic for the rapidly decreasing Born-Mayer potential that Λ' is relatively small. Seen from the scattering center, the interaction takes place within an angle (Fig. 9) $\Lambda'/p' = \sqrt{2\pi a'/p'}$ going to zero for $p' \gg a'$. For comparison we mention that the corresponding angle for the Coulomb potential is 90° for large p'. The potential at the end of the collision length is given by

$$\Phi'_{\text{end}} = A' \exp\left(- \frac{1}{a'} \sqrt{p'^2 + (\Lambda'/2)^2} \right) \approx A' e^{-p'/a'} \cdot e^{-\pi/4} \tag{4.4.5}$$

for $p'/a' \gg 1$, which is less than half of the potential in the closest approach.

So far, we required the MA to be valid. Let us now keep p' fixed and lower the energy so that we arrive at appreciable scattering angles, where the MA breaks down. As a first approximation, Λ' being defined as the real path length travelled during the collision remains independent of

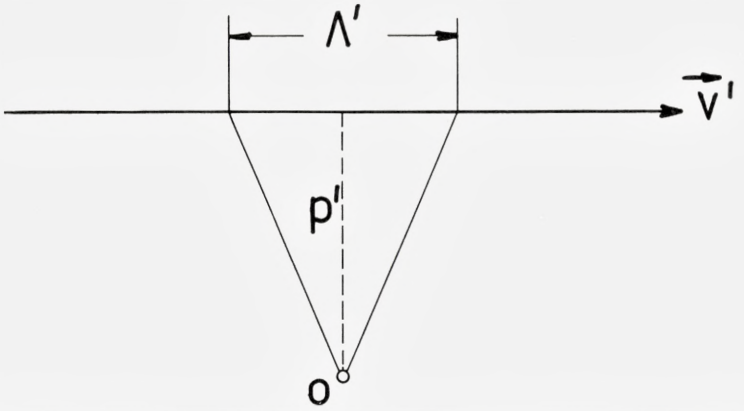

Fig. 9. The collision length Λ'. 0: scattering center. p': impact parameter. v': relative velocity.

energy; perhaps it will slightly decrease, since the particle is scattered away from the force field. Thus, we suppose that the relation

$$\Lambda' \lesssim \sqrt{2\pi a' p'} \tag{4.4.6}$$

should be valid even for large angle scattering.

Let us verify this by considering the opposite case, where p' is small. For $p' = 0$, one can solve the equation of motion exactly (LEHMANN & LEIBFRIED, 1961) with the result

$$\dot{r}' = v' \tanh \frac{v' t}{2a'}. \tag{4.4.7}$$

The velocity $\dot{r}'$ is zero in the closest approach ($t = 0$). From (4.4.7) we get a collision time

$$\Delta\tau' = 4a'/v' \tag{4.4.8}$$

and a corresponding path length

$$\Lambda' \approx 2a' \quad \text{for} \quad p' \approx 0, \tag{4.4.9}$$

as (4.4.7) represents, roughly, a uniformly accelerated motion within $|t| < 2a'/v'$.

Comparing the collision lengths (4.4.4) and (4.4.9) we find the unequality (4.4.6) being fulfilled, except for impact parameters $p'/a' < 2/\pi$, while a comparison of the corresponding collision times (4.4.3) and (4.4.8) gives discrepancies already at $p'/a' < 8/\pi$. So we conclude that Λ' is a well-

defined quantity, which for all impact parameters under consideration ($p'/a' \gtrsim 1$) may be majorized by (4.4.6).

We want to apply this result to our collision model within the range of applicability of the DCA. The corresponding path lengths in the elliptical potential can easily be found from the definitions in sect. 3.3, but the relation to laboratory quantities involves the so-called time integral. This quantity, which connects relative and centre-of-mass motion, is usually (LEHMANN & LEIBFRIED, 1961) derived for two-particle collisions but can easily be generalized to our situation. This is done in Appendix B. The coordinate system is chosen so that the origin is the initial ring center, and the time scale is such that the closest approach happens at $t = 0$. For $t \gg 0$, i. e. after the interaction, relative and center-of-mass motion obey the following equations:

$$\text{(B. 12)}: \quad r'(t) = \sqrt{p_D^2 + (sv_0 t + \tau_D)^2}. \tag{4.4.10}$$

$$\text{(B. 3) \& (B. 8)}: \quad X(t) = s^4 (v_0 t - \tau_D/s). \tag{4.4.11}$$

The time integral τ_D is given by (B. 9) and has been tabulated by ROBINSON (1963). The position of the projectile at $t = 0$ as well as the complete asymptotic motions $x_0(t)$, $x_1(t)$, $y_1(t)$ are listed in (B. 11) and (B. 14).

Finally, we are interested in the actual collision time $\Delta\tau$ corresponding to the path length (4.4.6). For not too large angles ($\vartheta < \pi/2$), $\Delta' = 2\,\overline{P_0 Q'}$ (Fig. 13 in appendix B) will approximately be equal to $2\overline{QQ'}$. Applying the cosine relation on the triangle $\overline{0QQ'}$ and inserting (4.4.10) and (4.4.4), we obtain

$$\Delta\tau = \frac{1}{sv_0}\left(\sqrt{2\pi a_D p_D} + 2p_D \operatorname{tg}\vartheta/2 - 2\tau_D\right). \tag{4.4.12}$$

For $\vartheta = 0$, τ_D goes to zero, so that $\Delta\tau$ goes over into $\Delta\tau'$ (4.4.3), as it must be. At finite angles, $\Delta\tau$ is greater than $\Delta\tau'$.

4.5 Validity of Approximations.

In this section we discuss the applicability of our four approximations within the model defined in 2.1. The limitations of the model itself will then be mentioned in the subsequent chapter.

In the following we assume scattering angles for a spherical potential to be given exactly, for example from Robinson's tables, so that the only approximative step consists in reduction to spherical symmetry. We shall first discuss the different approximations in terms of the reduced scattering angle ϑ.

From the construction we know that
i) the CCA yields the exact result for $\vartheta \approx \pi$. Furthermore from Appendix A,
ii) the MA is asymptotically exact for high energies (small ϑ).

Following the examples from sect. 4.3 we suggest:
I) The DCA is a good overall approximation.
II) For $s^4 \ll 1$ the validity of the MA is much better than in the corresponding two-particle collision.
III) For $s^4 \approx 1$, also the CVA is an excellent approximation

I. DCA. We first show that DCA and MA agree at high energies. Using the perturbation expansion

$$\vartheta = \frac{A_D}{E_r} \cdot \frac{p_D}{a_D} K_0(p_D/a_D) \approx \frac{A_D}{E_r} \cdot \sqrt{\frac{\pi}{2} \frac{p_D}{a_D}}\, e^{-p_D/a_D}, \tag{4.5.1}$$

and inserting (3.3.8) one obtains

$$\text{DCA:}\ \vartheta = \sqrt{\frac{Mm_0}{m_1^2}} \frac{A}{E_0} \sqrt{\frac{\pi}{2} \frac{L}{a}}\, e^{-L/a}. \tag{4.5.2}$$

For the MA we obtain from (A.7)

$$\text{MA:}\ \vartheta = ns^2 \frac{A}{E_r} \cdot \frac{sp}{a} K_0(sp/a) \approx \sqrt{\frac{Mm_0}{m_1^2}} \frac{A}{E_0} \sqrt{\frac{\pi}{2} \frac{L}{a}}\, e^{-L/a}, \tag{4.5.3}$$

in perfect agreement with (4.5.2). The second step in (4.5.1) using (2.2.3) is not exact as soon as p_D/a_D is not large ($s^4 \ll 1$). Numerically, ϑ_{DCA} is 10 pct. smaller than ϑ_{MA} at $p_D/a_D = 1$ and large E_0.

Next, we compare DCA and CCA at large ϑ. A convenient scattering formula near $\vartheta = \pi$ is found by expanding (4.1.5)

$$\cos \vartheta/2 = \frac{p'}{R_0'}(1 + a'/R_0'), \quad \text{for} \quad \vartheta \approx \pi, \tag{4.5.4}$$

where R_0' is defined in (4.1.6). Inserting (3.2.8) and (3.3.8) and neglecting a'/R_0' in (4.5.4) for low energy we get

$$\text{CCA:}\ \cos \vartheta/2 = \frac{s^2 L/a}{ln(MA/m_1E_0)}, \tag{4.5.5}$$

$$\text{DCA:}\ \cos \vartheta/2 = \frac{s^4 L/a}{ln(MA/m_1E_0) - \dfrac{nm_1}{M} L/a}. \tag{4.5.6}$$

Obviously, the two expansions only agree for $L/a \to 0$ and $s^4 = 1$. Otherwise both numerator and denominator in (4.5.6) are smaller than in (4.5.5) so that the numerical difference is not too big.

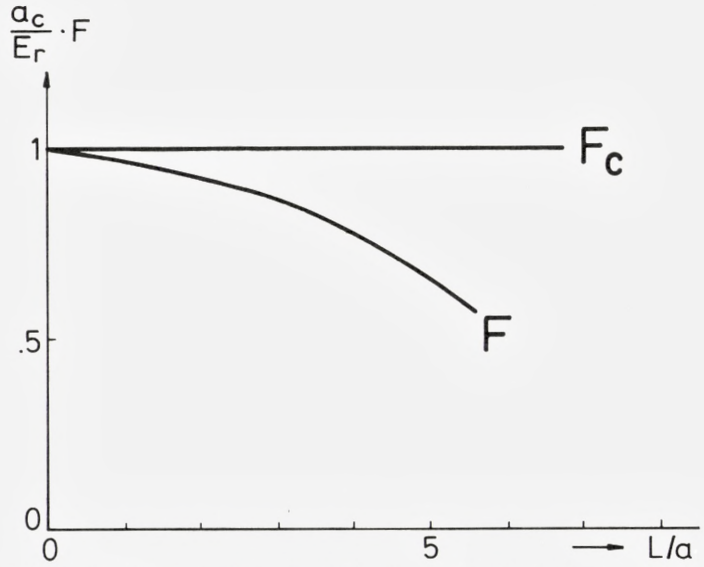

Fig. 10a. Magnitude of force in CCA. F = real force, F_C = CCA force.

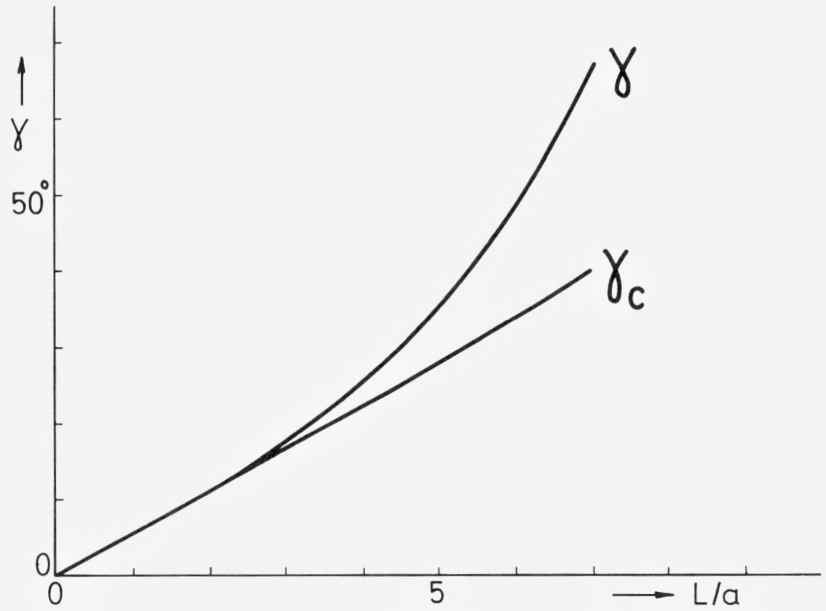

Fig. 10b. Angle of forces to the negative x-axis in CCA, γ = angle of the real force, γ_C = angle of the CCA force.

Fig. 10a–d. Comparison of real and approximate forces in the closest approach, for the example discussed in sect. 4.3 (Fig. 7); $s^4 = 1/3$, $E_0/A = 4.45_{10}{}^{-3}$.

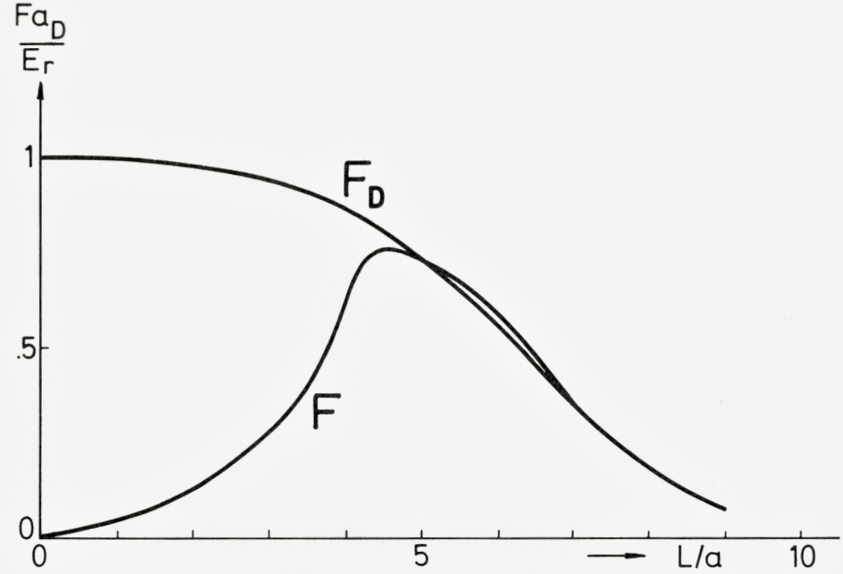

Fig. 10c. Magnitude of forces in DCA. F = real force, F_D = DCA force.

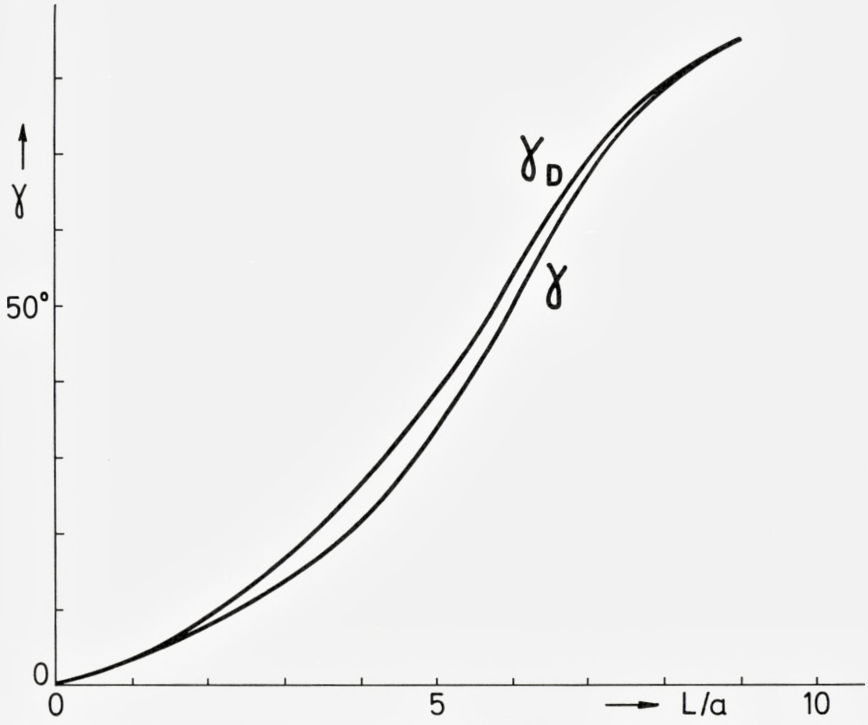

Fig. 10d. Angle of force to the negative x-axis in DCA. γ = angle of real force, γ_D = angle of DCA force.

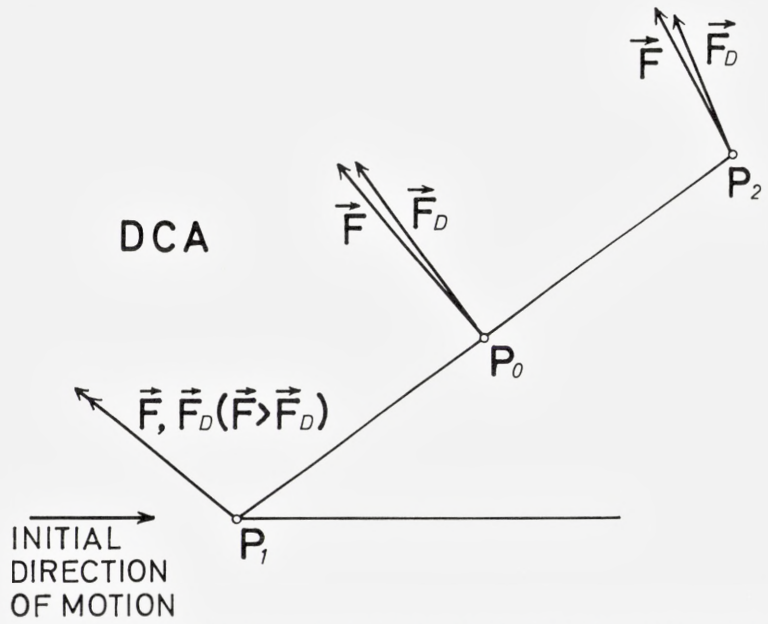

Fig. 11. Comparison of forces in three characteristic points within the collision length (see Fig. 13). $L/a = 6$; $s^4 = 1/3$; $E_0/A = 4.45_{10}{}^{-3}$.

At intermediate scattering angles both CCA and MA are suspect. To estimate the accuracy of the DCA we compare the actual, elliptic force field with the spherical one from the DCA in that region where deflection takes place, i. e. within the collision length. The most important point is, of course, the closest approach r'_m. In Fig. 10a–d we have plotted magnitude F and angle γ (measured with respect to the negative x-direction) of the real force $\vec{F}$ and the approximate forces $\vec{F}_C$ and $\vec{F}_D$ in the closest approach as calculated respectively by the CCA and the DCA. Fig. 10d shows that the direction of the force is very well approximated by the DCA at all impact parameters. The magnitude (Fig. 10c) is only correct at $L/a \gtrsim 5$, while it is drastically overestimated by the DCA at small L. This is immediately evident from the construction of the potential Φ_D (Fig. 5). The scattering angle ϑ is not affected very much by this discrepancy, but other quantities must be, for example the closest approach itself as well as time integral and collision length.

Figs. 10a and 10b show that the CCA force deviates considerably from the real force already at rather small values of L/a. This might explain the rather limited range of applicability of the CCA in Fig. 8. It means also that eq. (4.3.17) will in most cases be more adequate to determine E_{refl} than (4.3.16) or (4.3.19).

In order to estimate the accuracy of the DCA scattering angle at $L/a \approx 6$ we note that the errors of γ_D and F_D are around 5 pct., while the discrepancies of γ_C and F_C (Fig. 10a and b) are very large. Furthermore, the direction of the discre-

pancies indicates that the DCA underestimates ϑ, while CCA clearly overestimates. Hence, one would suppose that the DCA angle is about 5 pct. too small under the assumption that these relations are qualitatively the same within the whole collision length.

To be sure about this, we have also calculated the forces in two other points within the collision length, namely the points P_1 and P_2 from Fig. 13. It is easy to see that the length $\overline{P_1P_2}$ is not much smaller than Λ as defined by (4.4.4). The forces are shown in Fig. 11 for the case $L/a = 6$. P_0 is the closest approach (Fig. 13). Clearly, the discrepancies in P_1 and P_2 are not greater than in P_0.

We note that the validity of the DCA force field rapidly decreases, just as $\vartheta > \pi/2$. This seems evident from the construction of the potential (Fig. 5), as the particle is deflected far away from that point where we have matched the potential. We consider this result to be more general and assume in the following the DCA to be an accurate description of our model for $\vartheta \lesssim \pi/2$, except for $s^4 < 0.1$, where the error in ϑ might exceed 10 pct. At $\vartheta > \pi/2$, the scattering angle itself might be well approximated, but other quantities should be considered with care.

II. MA. We now investigate the error which is made by evaluating the DCA scattering angle by the MA. According to (4.5.2) and (4.5.3) this is equivalent to treating the original problem by the perturbation approach, for $s^4 > 0.1$.

Following LEHMANN & LEIBFRIED (1963), the error can be estimated from the proportion of second and first order contributions in the perturbation series

$$\vartheta = \vartheta^{(1)} + \vartheta^{(2)} + \ldots \tag{4.5.7}$$

to be

$$\left|\frac{\vartheta^{(2)}}{\vartheta^{(1)}}\right| = \frac{A_D}{E_r} \frac{\dfrac{p_D}{a_D} K_1\left(2\dfrac{p_D}{a_D}\right) - \dfrac{3}{2} K_0\left(\dfrac{p_D}{a_D}\right)}{K_0(p_D/a_D)} \approx \frac{A_D}{E_r} \cdot \frac{1}{\sqrt{2}} e^{-p_D/a_D}\left(\frac{p_D}{a_D} - 1.19\right). \tag{4.5.8}$$

In the second step we used the asymptotic expansion of the Hankel functions K_0 and K_1 (JAHNKE et al., 1960). Inserting (3.3.8) we get

$$\left|\frac{\vartheta^{(2)}}{\vartheta^{(1)}}\right| = \left(\frac{m_0}{m_1} + n\right) \frac{A}{E_0} \left(\frac{m_0}{M}\frac{L}{a} - 1.19\right) \frac{1}{\sqrt{2}} e^{-L/a}. \tag{4.5.9}$$

For the pure two-particle collision one would obtain

$$\left|\frac{\vartheta^{(2)'}}{\vartheta^{(1)'}}\right| = \left(\frac{m_0}{m_1} + 1\right) \frac{A}{E_0} \left(\frac{L}{a} - 1.19\right) \frac{1}{\sqrt{2}} e^{-L/a}. \tag{4.5.10}$$

Obviously, (4.5.9) and (4.5.10) are only equivalent for $m_0 \gg m_1$. Already for $m_0 \approx m_1$ there is a considerable difference, and for $m_0 \ll m_1$ one gets

$$\left|\frac{\vartheta^{(2)}}{\vartheta^{(1)}}\right| \approx \frac{A}{E_0} \left(\frac{m_0}{m_1}\frac{L}{a} - \frac{1.19}{n}\right) \frac{1}{\sqrt{2}} e^{-L/a}; \quad m_0 \ll m_1 \tag{4.5.9'}$$

instead of

$$\left|\frac{\vartheta^{(2)'}}{\vartheta^{(1)'}}\right| \approx \frac{A}{E_0}\left(\frac{L}{a} - 1.19\right)\frac{1}{\sqrt{2}}\, e^{-L/a} \tag{4.5.10'}$$

for the two-particle collision. For the example illustrated in Fig. 8 the error in the energy loss, which is twice the error in angle, is predicted to be

$$\frac{\delta(\Delta E)}{\Delta E} \leq \frac{31\ \text{eV}}{E_0} \tag{4.5.11}$$

by (4.5.9'), while (4.5.10') yields $114\ \text{eV}/E_0$. Comparison to Fig. 8 shows that the actual discrepancy between MA and DCA is even smaller than (4.5.11), as long as $E_0 > E_0(\max)$.

III. CVA.

We show that CVA and MA agree at high energies. Starting at (3.4.4) we obtain

$$\Delta E = n\Delta E_1 \approx \frac{m_1}{m_0} E_0 \cdot \alpha^2 = n\frac{m_0}{m_1}\frac{A^2}{E_0}\cdot\frac{\pi}{2}\frac{L}{a}\, e^{-2L/a}, \tag{4.5.12}$$

in agreement with (2.2.2), if only $L/a \gg 1$. This asymptotic behaviour is independent of the mass ratio, contrary to the DCA, which means that in the case $s^4 \ll 1$ the CVA is asymptotically exact, but a bad approximation at finite E_0, while the opposite holds for the DCA.

At $m_0 \gg m_1$, both DCA and CVA have the right asymptotic behaviour. In order to find the deviations at smaller energies, we consider the second order momentum approximation. Expanding both ϑ(DCA) and α(CVA) as well as the expressions for the energy loss (2.4.13) and (3.4.4) in powers of A, we obtain to the second order

$$\frac{\Delta E(\text{DCA})}{\Delta E(\text{CVA})} = \frac{1 + 2\vartheta^{(2)}/\vartheta^{(1)}}{1 + 2\alpha^{(2)}/\alpha^{(1)}} \approx 1 + 2\left(\frac{\vartheta^{(2)}}{\vartheta^{(1)}} - \frac{\alpha^{(2)}}{\alpha^{(1)}}\right). \tag{4.5.13}$$

$\vartheta^{(2)}/\vartheta^{(1)}$ is given in (4.5.9) apart from the sign: $\dfrac{\vartheta^{(2)}}{\vartheta^{(1)}} < 0$. $\alpha^{(2)}/\alpha^{(1)}$ is easily found using the definitions in sect. (3.4), so we obtain

$$\frac{\Delta E(\text{DCA})}{\Delta E(\text{CVA})} = 1 + 1.19\sqrt{2}\,\frac{nAe^{-L/a}}{E_0}, \quad \text{for large } E_0. \tag{4.5.14}$$

(4.5.14) is independent of the mass ratio but only correct for $\dfrac{m_0}{M}\dfrac{L}{a} \gg 1$. It is seen that the CVA underestimates ΔE, which is to be expected, as the CVA underestimates the collision time.

For numerical estimates one should remember that (4.5.14) is only valid within the radius of convergence of the perturbation series.

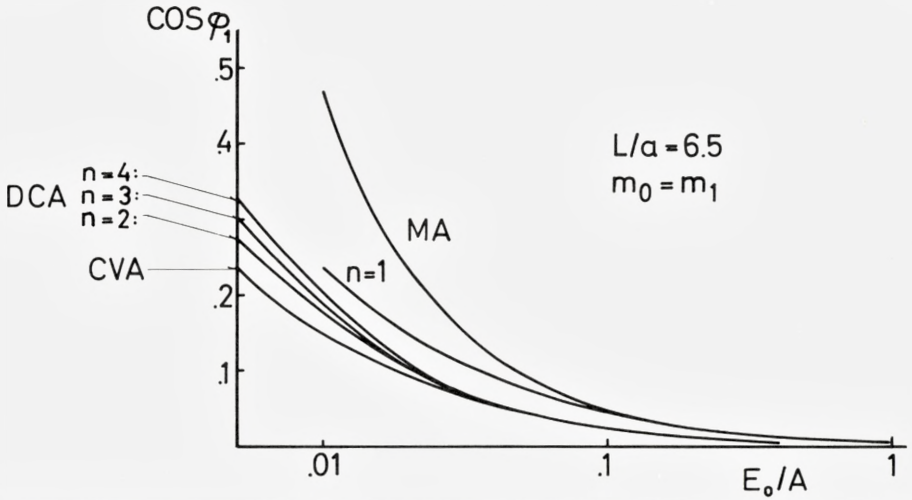

Fig. 12a. Starting angle φ_1 of ring particle 1 as a function of projectile energy for different numbers of ring atoms (n = 2, 3, 4), compared to n = 1 (pure two-particle scattering), MA and CVA.

4.6 Angular relations

It would be of considerable interest also to investigate many-body scattering events which are not as symmetrical as the model discussed until now. It is immediately evident that most of the techniques applied in the present paper are rather specific for the symmetric ring collision and cannot be generalized in a straightforward manner.

If we confine ourselves to distant collisions it will always be reasonable to apply the MA above some well-defined limiting energy. At low energies, it will often happen that the path of the projectile may be well approximated by a straight line, even if the relative energy transfer to atoms surrounding the path is not small, just because of the stabilizing effect of an assembly of scattering centers. In these cases, it seems most reasonable to apply the CVA in order to calculate the transferred energy, rather than to resolve all interactions into two-body events and treat these by familiar scattering theory.

Applying the CVA to a given scattering problem, one obtains energies and directions of motion for all the struck particles. From that, using conservation laws, one might also get the total energy and momentum change of the projectile. This procedure has been used by WEIJSENFELD (1964) in the theory of assisted focusing collision sequences. The validity of the approach has not been estimated.

From our model, it is only possible to estimate the accuracy of the CVA in the completely symmetrical case, where the assumptions underlying the CVA are best satisfied. As to the calculation of transferred energies, this has been done in the preceding section. In order to see that the situation is quite analogous with respect to angular relations, we just discuss an example. In Fig. 12a, we have plotted the cosine of the starting angle φ_1 of ring particle 1 for different approximations and various numbers of ring atoms. The CVA claims that φ_1 is independent of n. Within the DCA, the angle φ_1 appears to be almost identical for n = 2, 3 and 4.

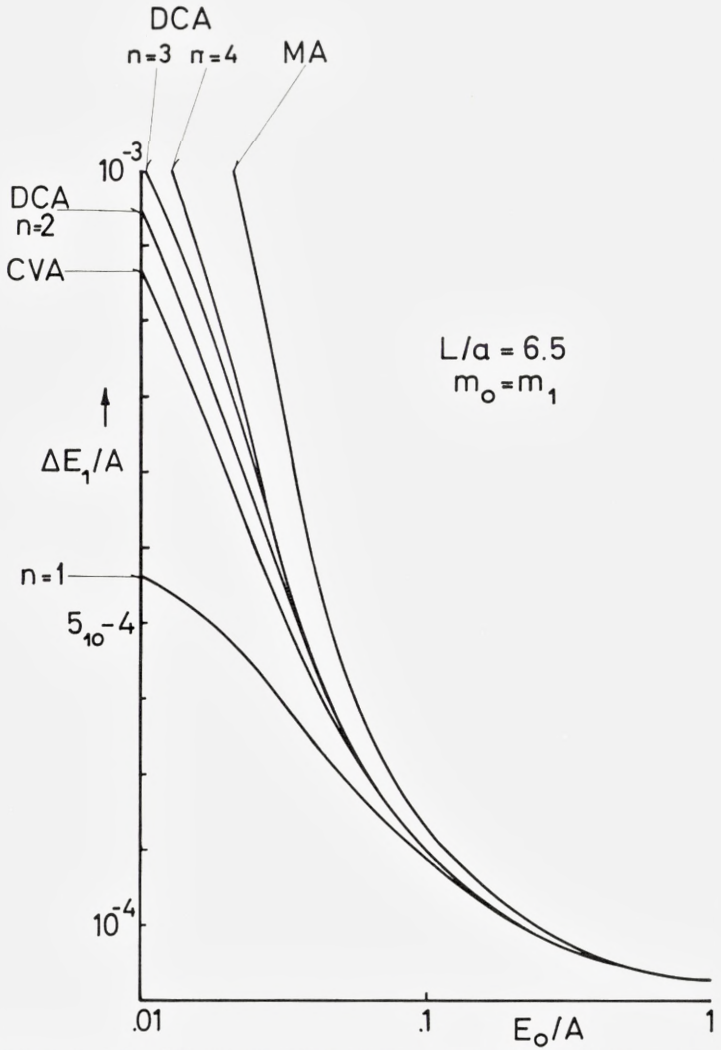

Fig. 12b. Energy transfer ΔE_1 to one ring atom corresponding to the angles in Fig. 12a.

In the energy region where the MA fails completely, the scattering angle calculated from the assumption of pure two-particle scattering ("$n = 1$") appears still to be a satisfactory approximation[1]. This is not the case if one considers the energy

[1] Note that for large E

$$\cos\varphi_1\Big|_{\text{2-body}} = \left(1 + \frac{m_1}{m_0}\right)\cos\varphi_{1\,\text{CVA}},$$

due to the violation of momentum conservation in x-direction. In applications, this discrepancy is unimportant.

ΔE_1 transferred to one ring atom (Fig. 12b). Here, the two-particle approach fails completely. One might suppose that the relations between the different approaches as indicated in Fig. 12a and b are more general, but a detailed investigation is outside the scope of this paper.

§ 5. Limitations of the Model

5.1 Validity of classical scattering

A detailed investigation of the limitations of classical scattering due to the uncertainty principle would require a wave packet description of our model. This requires in turn some knowledge of the classical orbits in the case of deviations from perfect symmetry which are not considered in this paper.

In order to get a feeling for the magnitude of quantum corrections to our model, we estimate the accuracy of ΔE_1 and ΔE only in the special case of a heavy projectile ($m_0 \gg m_1$) and small energy transfer, where the main uncertainty arises from localizing the ring particles, so that the projectile may be considered to have well-defined position and momentum.

The uncertainty in the scattering angle α of one ring particle in a system moving with velocity v_0 (Fig. 6) is calculated by the method of Bohr (1948) modified for Born-Mayer scattering. Assuming

$$\partial\alpha/\partial L \approx -\alpha/a, \tag{5.1.1}$$

one obtains the relative uncertainty

$$\frac{\delta\alpha}{\alpha} = \sqrt{\frac{\lambda\!\!\!^{-}_1}{a\alpha}}, \tag{5.1.2}$$

where

$$\lambda\!\!\!^{-}_1 = \frac{\hbar}{m_1 v_0}. \tag{5.1.3}$$

As α determines the energy transfer, we obtain from (3.4.4)

$$\frac{\delta(\Delta E_1)}{\Delta E_1} = 2\frac{\delta\alpha}{\alpha} = \left[\frac{8\hbar^2}{a^2 m_1 \Delta E_1}\right]^{1/4} \tag{5.1.4}$$

for the relative uncertainty in ΔE_1.

Finally, since the different ring particles are independent of each other, the uncertainty in the total energy loss ΔE is given by

$$\frac{\delta(\Delta E)}{\Delta E} = n^{-1/2} \cdot \frac{\delta(\Delta E_1)}{\Delta E_1} = n^{-1/4} \cdot \left(\frac{8\hbar^2}{a^2 m_1 \Delta E} \right)^{1/4}. \tag{5.1.5}$$

Assuming $a = 0.2$ Å one obtains from (5.1.5)

$$\frac{\delta(\Delta E)}{\Delta E} = \left(\frac{0.8\text{eV}}{n A_1 \Delta E} \right)^{1/4}, \tag{5.1.6}$$

where A_1 is the mass number. As the energy at which the fraction (5.1.6) becomes comparable to 1 usually lies in the range of validity of the MA, one might suppose that the classical approach should be successful below this limit, also at energies where the MA breaks down.

The relations (5.1.4) and (5.1.5) remain qualitatively correct even for $m_0 \lesssim m_1$, as long as the energy loss is small. But in the energy region where the projectile can be reflected, these considerations might be insufficient.

One should mention that the limiting energies calculated by Lehmann & Leibfried (1963) are considerably higher than those arising from (5.1.4) or related equations. This is due to the fact that the criterion of Williams (1945) used by these authors in the case of screened potentials is only a necessary condition for the applicability of classical orbit pictures.

5.2 Inelasticity

Due to ionization and excitation of electrons the collisions in a crystal are not perfectly elastic. It has often been assumed that a certain ionization threshold energy E_I exists below which inelastic effects should be negligible. It seems well-established that such a general threshold in the sense of a cut-off energy does not exist. Nevertheless, there might be a characteristic energy separating those regions, where, respectively, elastic and inelastic effects dominate, but this energy will in general depend in a sensitive way on the considered effect.

In this paper we are concerned with particle velocities much smaller than $e^2/\hbar$, so that dipole resonance excitation will not take place (Bohr, 1948). One only deals with close Coulomb encounters of the projectile with the electrons of the crystal. Seitz (1949) assumed that these will not lead to excitation if the maximum energy transfer is smaller than the Fermi energy in a metal or the ionization energy in an insulator. The theory for stopping of charged particles in an electron gas (Lindhard, 1954) does not confirm this statement. The stopping power turns out to be proportional to velocity:

$$\left(\frac{dE}{dx} \right)_e = \text{const} \cdot v, \tag{5.2.1}$$

the proportionality constant depending on the charge of the projectile and the density of the electron gas. Within the limits of applicability of the Thomas-Fermi

model eq. (5.2.1) should also be valid for non-uniform electron gases as they occur in solids and, especially, in metals.

As electronic stopping acts only as a minor correction on the orbit of the projectile, it seems to be a reasonable approximation to treat the collision as being elastic and to add the inelastic contribution later on, provided the proportionality constant in (5.2.1) can be calculated. Electronic stopping may be dominating at energies considerably below the ionization limit, especially in channelled motion.

5.3 Effect of binding forces

In our scattering model it is an essential assumption that the ring atoms are not bound by external forces or interact with one another. In a crystal, however, the atoms are bound to their lattice sites by oscillator forces, as a first approximation.

It has been shown by BOHR (1913, 1948) that oscillator forces can be neglected in collision problems if the collision time $\Delta\tau$ obeys the condition

$$\omega_1 \Delta\tau < 1, \tag{5.3.1}$$

where ω_1 is the oscillator frequency of the struck particle. Eq. (5.3.1) defines an adiabatic limit. For $\omega_1 \Delta\tau > 1$, the energy loss is overestimated by assuming free scattering.

As the collision time increases with decreasing energy, our description can only be correct above some limiting energy which turns out to be quite small.

For $\Delta\tau$ we use, for not too small s^4 and $\vartheta \ll \pi/2$, the first term in (4.4.12), so

$$(\Delta\tau)^2 \approx \frac{2\pi a_D p_D}{(sv_0)^2} = \frac{2\pi a L}{v_0^2}. \tag{5.3.2}$$

The frequency ω_1 is conveniently found from the coupling constants of the lattice by assuming all atoms fixed except 1. If we only take nearest neighbour interaction into account, we get

$$\text{for the FCC lattice: } m_1\omega_1^2 \approx 4(\alpha + 2\beta) \tag{5.3.3}$$

$$\text{and for the BCC lattice: } m_1\omega_1^2 \approx 8\alpha, \tag{5.3.4}$$

where α and β are coupling constants in the notation of LEIBFRIED (1955). Hence, (5.3.1) reads

$$\left.\begin{aligned} & 4\pi \frac{m_0}{m_1} \frac{aL(\alpha + 2\beta)}{E_0} < 1 \quad \text{for FCC lattice,} \\ \text{and} \quad & \\ & 8\pi \frac{m_0}{m_1} \frac{aL\alpha}{E_0} < 1 \quad \text{for BCC lattice.} \end{aligned}\right\} \tag{5.3.5}$$

As an example, we discuss the ⟨100⟩ focuson in Cu considered by WEIJSENFELD (1964). Here, we have (JACOBSEN, 1955)

$$\alpha = .30 \text{ eV/Å}^2; \quad \beta = .54 \text{ eV/Å}^2. \tag{5.3.6}$$

For $L/a = 10$, $a = .2$ Å and $m_0 = m_1$ we obtain

$$\omega_1 \Delta\tau = \left(\frac{7 \text{ eV}}{E_0}\right)^{1/2}, \tag{5.3.7}$$

so that the condition (5.3.1) is fulfilled at $E_0 > 7$ eV. As this energy is of the order of the potential barrier, the energy limits for reflection and penetration, as defined in (4.3.16) etc., will suffer some modifications. The ΔE vs. E_0 curves around and above $E_0(\max)$ will not be affected.

Appendix A

Perturbation Expansion

Eq. (3.1.2) can in principle be solved by a perturbation series

$$y(x) = y^{(0)}(x) + y^{(1)}(x) + \ldots . \tag{A 1}$$

in powers of the potential, Φ. We write (3.1.2) in the form

$$\frac{1}{2}(\Phi_y - y'\Phi_x)(1 + y'^2) + (E_r - \Phi)y'' = 0. \tag{A 2}$$

Φ_x and Φ_y indicating partial derivatives. The zero order term yields

$$E_r y^{(0)\prime\prime}(x) = 0; \quad y^{(0)\prime}(x) = \text{const.} = 0; \quad y^{(0)}(x) = \text{const.} = p; \tag{A 3}$$

Collecting first order terms we obtain

$$\frac{1}{2}\Phi_y(x,p) + E_r y^{(1)\prime\prime} = 0$$

or, using (2.4.8)

$$y^{(1)\prime\prime} = -\frac{nps^2}{2E_r}\,\frac{V'(\sqrt{x^2/s^2+s^2p^2})}{\sqrt{x^2/s^2+s^2p^2}}\,. \tag{A4}$$

where V' is the derivative of V with respect to the argument.

The scattering angle ϑ (fig. 3) in first order is given by

$$(\mathrm{tg}\,\vartheta)^{(1)} = y^{(1)\prime}(x=\infty) = \int_{-\infty}^{+\infty} dx\, y^{(1)\prime\prime}(x)$$

$$= -\frac{nps^3}{E_r}\int_{sp}^{\infty}\frac{V'(\eta)d\eta}{\sqrt{\eta^2-s^2p^2}}\,, \tag{A5}$$

where we have made the substitution

$$x^2/s^2 + s^2p^2 = \eta^2. \tag{A6}$$

For Born-Mayer interaction

$$V(\eta) = Ae^{-\eta/a} \tag{A7}$$

(A5) yields

$$(\mathrm{tg}\,\vartheta)^{(1)} = ns^2\cdot\frac{A}{E_r}\cdot\frac{sp}{a}\,K_0(sp/a). \tag{A8}$$

For small $\vartheta^{(1)}$, we write

$$(\mathrm{tg}\,\vartheta)^{(1)} \approx \vartheta^{(1)} \approx 2\sin\vartheta^{(1)}/2,$$

so (2.4.13) reads

$$\Delta E \approx 4\frac{nm_1}{M}E_0(\vartheta^{(1)}/2)^2 \approx n\frac{m_0}{m_1}\frac{A^2}{E_0}\left[\frac{L}{a}K_0\left(\frac{L}{a}\right)\right]^2, \tag{A9}$$

where we have used (2.4.9), (2.4.11) and (2.4.7). Eq. (A9) agrees with (2.2.2), as it must be.

Collecting second order terms in (A2) we obtain

$$\frac{1}{2}y^{(1)}\Phi_{yy}(x,p) - \frac{1}{2}y^{(1)\prime}\Phi_x(x,p) - y^{(1)\prime\prime}\Phi(x,p) + y^{(2)\prime\prime}E_r = 0$$

or, after partial integration,

$$(\mathrm{tg}\,\vartheta)^{(2)} = y^{(2)\prime}(\infty) = -\frac{1}{2E_r}\int_{-\infty}^{\infty} dx\, y^{(1)}(x)\,(\Phi_{yy}(x,p) - \Phi_{xx}(x,p)). \tag{A10}$$

As explained in sect. 3.1, there is no need to evaluate (A10) explicitly.

Appendix B

The time integral

Let the laboratory coordinates (2.4.1) satisfy the initial conditions

$$x_0(t_0) = \xi_0 < 0; \quad x_1(t_0) = 0; \quad y_1(t_0) = L \tag{B1}$$

and

$$\dot{x}_0(t_0) = v_0; \quad \dot{x}_1(t_0) = \dot{y}_1(t_0) = 0. \tag{B2}$$

From the definition (2.4.2) we get immediately the center-of-mass motion

$$X(t) = X(t_0) + \dot{X}(t_0)(t - t_0) = \frac{m_0}{M}\left(\xi_0 + v(t - t_0)\right). \tag{B3}$$

For the relative coordinates x, y (2.4.4) we obtain

$$\left.\begin{aligned} x(t_0) &= s\xi_0; \quad y(t_0) = L/s = p \\ \dot{x}(t_0) &= sv_0; \quad \dot{y}(t_0) = 0. \end{aligned}\right\} \tag{B4}$$

Integration of the equations of motion is possible for spherical potentials. Hence, we go over into the coordinate system (x', y') defined by the DCA, where (Fig. 5)

$$x' = x; \quad y' = y - y_D = y - p(1 - s^4). \tag{B5}$$

Here,

$$\left.\begin{aligned} x'(t_0) &= s\xi_0; \quad y'(t_0) = s^4 p = p_D \\ \dot{x}'(t_0) &= sv_0; \quad \dot{y}'(t_0) = 0. \end{aligned}\right\} \tag{B6}$$

With the potential $\Phi_D(r')$ from (3.3.4) we get

$$\frac{dr'}{dt} = \pm sv_0\left(1 - \frac{\Phi_D(r')}{E_r} - \frac{p_D^2}{r'^2}\right)^{1/2} \quad \text{for} \quad t \gtrless 0, \tag{B7}$$

where $r'^2 = x'^2 + y'^2$.

The closest approach is assumed at $t = 0$. Hence, $t_0 < 0$. Integration from t_0 to $t = 0$, assuming that the potential energy at $t = t_0$ is negligible, yields

$$sv_0 t_0 = \tau_D + x'(t_0) = \tau_D + s \cdot \xi_0, \quad \text{for} \quad t_0 \ll 0. \tag{B8}$$

Here τ_D is the "time integral"

$$\tau_D = (r_m'^2 - p_D^2)^{1/2} - \int_{r_m'}^{\infty} dr' \left\{\left(1 - \frac{\Phi_D(r')}{E_r} - \frac{p_D^2}{r'^2}\right)^{-1/2} - \left(1 - \frac{p_D^2}{r'^2}\right)^{-1/2}\right\}, \tag{B9}$$

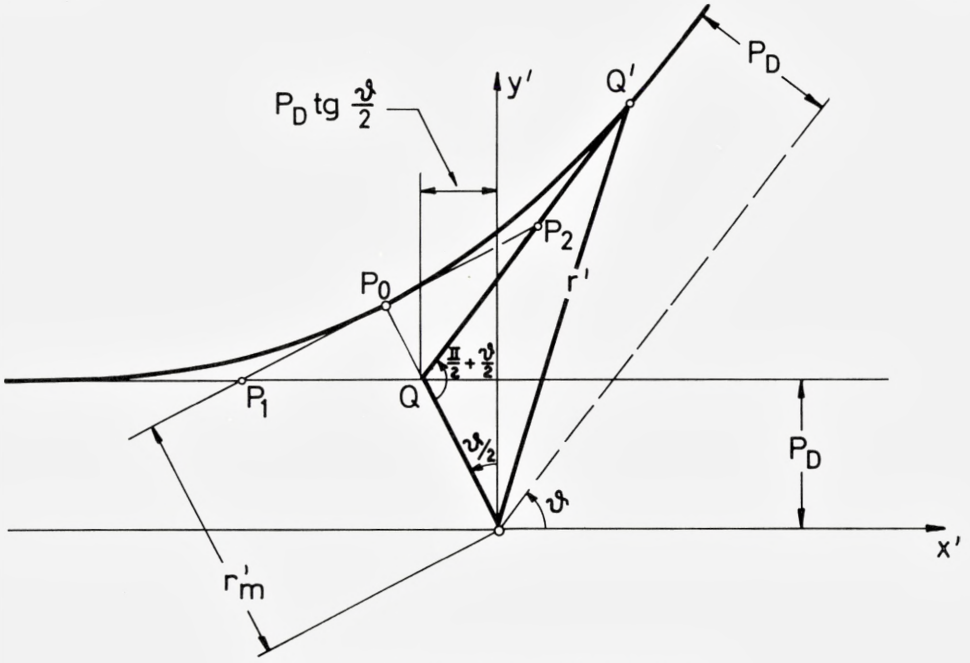

Fig. 13. Asymptotic orbits in reduced system.

which has been tabulated by ROBINSON (1963), and r'_m is the closest approach. From (B3) and (B8) we get the position of the centre-of-mass at $t = 0$:

$$X(0) = s^4(\xi_0 - v_0 t_0) = -s^3\tau_D. \tag{B10}$$

As

$$x'(0) = -r'_m \sin \vartheta/2,$$

the position of the projectile at the time of closest approach becomes

$$x_0(0) = X(0) + (1 - s^4)\frac{1}{s}x'(0) = -s^3\tau_D - (1 - s^4)\frac{r'_m}{s}\sin \vartheta/2, \tag{B11}$$

where use has been made of (2.4.5). Furthermore, for $t \gg 0$, we get in the same way as (B8)

$$sv_0 t = -\tau_D + \sqrt{r'^2 - p_D^2}; \quad \text{for} \quad t \gg 0. \tag{B12}$$

This relation governs the asymptotic orbits. We have (Fig. 13) for $t \gg 0$

$$y' = x' \operatorname{tg} \vartheta + \frac{p_D}{\cos \vartheta},$$

and x' and y' can be expressed by r':

$$\left.\begin{aligned} x' &= -p_D \sin \vartheta + \cos \vartheta \cdot \sqrt{r'^2 - p_D^2} \\ y' &= p_D \cos \vartheta + \sin \vartheta \sqrt{r'^2 - p_D^2}. \end{aligned}\right\} \qquad \text{(B13)}$$

Using eqs. (2.4.5), (B12) and (B13) one obtains

$$\left.\begin{aligned} x_0(t) &= (v_0 t + \tau_D/s)\left(1 - 2\frac{nm_1}{M}\sin^2 \vartheta/2\right) - s^3\left(2\tau_D + \frac{nm_1}{M} p \sin \vartheta\right); \\ x_1(t) &= (v_0 t + \tau_D/s) \cdot 2\frac{m_0}{M}\sin^2 \vartheta/2 - s^3\left(2\tau_D - \frac{m_0}{M} p \sin \vartheta\right); \\ y_1(t) &= (v_0 t + \tau_D/s) \cdot s^2 \sin \vartheta + sp\left(1 - 2\frac{m_0}{M}\sin^2 \vartheta/2\right), \end{aligned}\right\} \qquad \text{(B14)}$$

for $t \gg 0$.

Acknowledgments

The main part of this work has been done at Strandkrogen, Fakse Ladeplads. The fruitful research atmosphere provided by Pia and Nina Sigmund and Agnete Andersen is gratefully acknowledged.

Many points have been clarified in discussions with our colleagues at Aarhus and Risö. Our sincere thanks are to professor Jens Lindhard for many critical remarks and for introducing to us the problems discussed in sections 5.1 and 5.2, and to Mrs. V. Nielsen for critically reading the paper.

We acknowledge the careful assistance of Miss Susann Toldi in the preparation of various versions of the manuscript.

Part of this work was supported by a NATO fellowship provided by Deutscher Akademischer Austauschdienst (PS) and a fellowship from the Technical University of Copenhagen (HHA).

Hans Henrik Andersen
Physics Department
Atomic Energy Commission
Research Establishment Risø
Roskilde, Denmark.

Peter Sigmund
Institute of Physics, University of Aarhus
Aarhus, Denmark.

Present adress:
Institut für Reaktorwerkstoffe
Kernforschungsanlage
Jülich, Germany.

References

H. H. Andersen – P. Sigmund, 1965 a: Phys. Lett. **15**, 237.
1965 b: Risö Report No. 103.
N. Bohr, 1913: Phil. Mag. (6) **25**, 10.
1948: Mat. Fys. Medd. Dan. Vid. Selsk. **18**, no. 8.
J. A. Brinkmann, 1954: J. Appl. Phys. **25**, 961.
J. B. Gibson – A. N. Goland – M. Milgram – G. H. Vineyard, 1960: Phys. Rev. **120**, 1229.
D. Heinrich, 1964: Ann. Phys. **13**, 284.
E. H. Jacobsen, 1955: Phys. Rev. **97**, 654.
E. Jahnke – F. Emde – F. Lösch, 1960: Tafeln höherer Funktionen, Stuttgart.
G. Leibfried, 1955: Handbuch der Physik, Bd. VII/1 (Springer Verlag).
G. Leibfried – O. S. Oen, 1962: J. Appl. Phys. **33**, 2257.
C. Lehmann – G. Leibfried, 1961: Z. Phys. **162**, 203.
1963: Z. Phys. **172**, 465.
C. Lehmann – M. T. Robinson, 1964: Phys. Rev. **134** A, 37.
J. Lindhard, 1954: Mat. Fys. Medd. Dan. Vid. Selsk. **28**, no. 8.
M. T. Robinson, 1963: ORNL-3493.
M. T. Robinson – O. S. Oen, 1963: Phys. Rev. **132**, 2385.
F. Seitz, 1949: Disc. Far. Soc. **5**, 271.
P. Sigmund – P. Vajda, 1964: Risö Report No. 84.
C. H. Weijsenfeld, 1964: preprint to be published.
E. J. Williams, 1945: Rev. Mod. Phys. **17**, 217.

Indleveret til Selskabet den 17. august 1965.
Færdig fra trykkeriet den 3. marts 1966.